WEALTH FROM OCEANS FLAGSHIP
www.csiro.au

What are the important thresholds and relationships to inform the management of Crown-of-Thorns Seastar

CSIRO-GBRMPA partnership

Russ Babcock, Éva Plagányi, E. Bee Morello, Wayne Rochester

Partnership project with

Jessica Hoey, GBRMPA,
Morgan Pratchett, James Cook University
Ken Anthony, AIMS

30 June 2014

Client: GBRMPA
Client contact: Jessica Hoey

Australian Government
Great Barrier Reef
Marine Park Authority

Commonwealth Scientific and Industrial Research Organisation

Wealth from Oceans Flagship

Citation

Babcock, R., Plagányi, É., Morello, E.B., Rochester, W. 2014. What are the important thresholds and relationships to inform the management of COTS? Draft report, 30 June 2014. CSIRO, Australia.

Copyright and disclaimer

CSIRO thanks the Great Barrier Reef Marine Park Authority, the Queensland Government, the Association of Marine Park Tourism Operators and all contributors to the Integrated Eye on the Reef Program for the provision of data associated with reef health and crown-of-thorns starfish.

Important disclaimer

Contents

Figures

Tables

Acknowledgments

CSIRO thanks the Great Barrier Reef Marine Park Authority, the Queensland Government, the Association of Marine Park Tourism Operators and all contributors to the Integrated Eye on the Reef Program for the provision of data associated with reef health and crown-of-thorns starfish. This work was supported by Great Barrier Reef Marine Park Authority (GBRMPA), and the CSIRO Wealth from Oceans Flagship. We acknowledge with thanks data provided by the Australian Institute of Marine Science (AIMS) (Long Term Monitoring Program data) and GBRMPA. We thank the following for providing data to inform our study: Hugh Sweatman (AIMS), Jessica Hoey (GBRMPA), Dave Fisk, Lyle Vail (Lizard Island Research Station).

Executive summary

The crown-of-thorns seastar (COTS), *Acanthaster planci*, is one of the main contributors to declines in coral cover on the Great Barrier Reef (GBR), and remains one of the major acute disturbances on coral reefs throughout much of the Indo-Pacific.

The aim of this project is to investigate important ecological thresholds and relationships to inform the management of COTS. To do this we use a range of modelling methods as well as analyses of all available empirical data.

Data from the management program removals of COTS provide near-real-time CPUE (Catch-Per-Unit-Effort) data that can be used to inform management. However CPUE data must be converted to density estimates before they can be related to ecological status of reefs or incorporated into ecological models. We developed a preliminary CPUE-COTS density relationship using data collected at Lizard Island by Fisk and Power (1999). A more accurate CPUE was then computed by using the size structure of management program removal data provided by GBRMPA to try and estimate what proportion of 1 year-old COTS (those we classified as younger than 2 years; 0.1 – 15 cm) are visible and hence culled. Using the management program removal data and our MICE model (Morello et al. in press), we estimated that the selectivity of the 1 yr-old animals is 19%, i.e. on average, we estimate that divers find and remove 19% of these smaller/younger animals, and we use this to convert model CPUE estimates to equivalent field measurements.

Building on this and on the results of Plagányi et al. (in press) we estimated an ecological threshold for COTS populations based on intrinsic birth and death rates. The critical ecological threshold levels for COTS population growth were estimated as density of 7.1 (±2.3) COTS ha^{-1} which equates to a COTS (removal) CPUE value of 0.028 (±0.01) COTS/min or below, that would be required to prevent or disrupt population growth. In terms of a COTS outbreak cycle, this is the point below which there is an abrupt decline in COTS such that the population is unable to sustain itself (occurring at a low coral cover of approximately 14%). Alternatively, a growing population at densities below this level would be unlikely to outbreak, regardless of the level of coral cover.

Model equations and best fit parameter estimates (following Morello et al. in press) were used to determine the threshold level of COTS that kept growth of fast growing corals in equilibrium (i.e. prevented coral from growing and recovering). These thresholds differed for different base levels of average coral cover. The model steady state analysis suggests that if coral cover is high, then the same number of COTS will have less impact on the system than for lower levels of coral cover. For cover of fast growing coral ('Coralf') in the range 20% to 50%, there was excellent agreement between these results and the outbreak threshold (10 COTS ha^{-1}) defined by Keesing and Lucas (1992).

For coral cover in the range 20-40%, our preliminary results suggest that the COTS CPUE should be maintained below approximately 0.05-0.06 COTS/min to keep the coral cover stable at current levels. Average coral cover is 35% (±17% SD) at reefs within the management program scope, with range 3-88%, suggesting that on average CPUE target rates should be less than 0.06 COTS/min (of 2+ & 19% 1 individuals) individuals. For areas with low coral cover (<20%), CPUE target rates should be lower, down to around 0.04 COTS/min. This compares well with the current management rules being implemented by GBRMPA and AMPTO as follows:

> Coral cover over 40% - keep CPUE <=0.1 COTS/min (this study suggests 0.07-0.09 COTS/min)
>
> Coral cover approaching 20%, keep CPUE <=0.05 COTS/min (this study suggests 0.04 COTS/min)

These results also provide scientific support for the current strategy to manage COTS below a conservative CPUE threshold when coral cover is less than 40%. Results are preliminary and may be refined as further data and information become available.

To complement the above equilibrium (static) analysis, we also used a spatially expanded version of our dynamic COTS model (Morello et al., in press) to evaluate the effect of manual lethal injections of different proportions of age 1 yr-old (0.1 – 15 cm) and age 2+ (> 15 cm) COTS at different levels of coral cover. The results show that both the proportion of COTS removed and initial coral cover have a substantial effect on the average number of years taken for fast-growing coral to recover. Moreover, progressively increasing the selectivity of 1+ COTS (i.e. proportion available for removal) and the proportion of total COTS removed, proportionally decreases the effects COTS have on coral.

Lastly, we use a COTS fertilisation model, parameterised with field data, to explore the relationship between COTS density and the reproductive potential of the population. The essence of these hypotheses is that if COTS aggregate for any reason, for example around residual food sources after events such as cyclones, or at high population densities, their reproductive success may increase greatly. Hence we examine whether there is a critical COTS density below which fertilisation fails, as this aids further in quantifying the density at which COTS remain at sub-outbreak compared with outbreak levels.

The results of the modelling, while still preliminary, show reasonable levels of comparability with observations of natural spawning (Babcock and Mundy 1993). The results of the model have important implications for management of COTS because they suggest that there is an Allee effect, which is a non-linear relationship between COTS abundance and zygote (larval) production, such that larval production increases faster than expected once density exceeds certain critical values. This means that if COTS density can be reduced below critical levels, then there is a substantially greater probability of recruitment failure because population-level reproductive output and the likelihood of further outbreaks declines more rapidly than indicated by density. The threshold level for zygote production appears to be at spawning densities of around 13-18 COTS where zygote production begins to increase rapidly. This was somewhat higher than the 7-9 age 2+COTS ha^{-1} threshold density below which management programs should keep COTS to maintain and improve coral cover. Therefore, if management actions can control COTS below the threshold levels to support coral recovery, they are also likely to impact on a COTS reproductive success.

In summary, modelling of COTS population reproductive success suggests that there may be thresholds in reproductive success that could be used to achieve more effective management of COTS populations on the GBR. These applications could relate to both active management (culling) situations but also in the broader context of monitoring and awareness of incipient outbreak conditions. The quantitative accuracy of these thresholds is critical to their application and we suggest a discrete set of further modelling simulations and empirical measurements that would increase certainty around these thresholds, independent from those considered above.

1 Introduction and Overview

The crown-of-thorns seastar (COTS), *Acanthaster planci*, is one of the main contributors to declines in coral cover on the Great Barrier Reef (GBR), and remains one of the major acute disturbances on coral reefs throughout much of the Indo-Pacific.

The aim of this project is to explore important ecological thresholds for COTS populations in relation to potential for population growth, available food sources (coral cover) and reproductive success. Knowledge of these thresholds will inform the management of COTS, which includes a comprehensive surveillance and management program. To do this we used a range of modelling methods as well as analyses of all available empirical data.

We thus tackle this problem from a number of different perspectives, summarised in a series of Chapters. We commence by drawing on the results of Plagányi et al. (in press) to estimate an ecological threshold for COTS, being the point where COTS densities cause an abrupt change in the ecosystem. We derive the minimum level of coral cover (and corresponding COTS density) below which a COTS population will decline abruptly (i.e. starve). This provides two insights, firstly the minimum level of coral below which COTS will starve, and secondly the minimum level of coral cover that needs to be maintained to enable a coral reef to recover from COTS predation.

Our next analysis takes into account that COTS are impacting a range of sites that have different (and often much higher) coral cover, and focuses on estimating the point at which the net growth rate in coral cover is zero. In other words, for a given coral cover, we estimate (based on our multispecies model), the COTS density that corresponds to the sub-outbreak threshold i.e. at lower COTS densities, the net coral growth rate exceeds COTS consumption and hence the COTS are not considered to be outbreaking. We compare model results with empirical findings and utilise the management program removal data for comparison.

In all cases, there is a need to convert the COTS density estimates to CPUE measures so that they can be directly compared with, or applied, in the field. Hence this report also summarises a preliminary method for deriving a COTS density – CPUE relationship. We use the management program size structure data provided by GBRMPA to estimate what proportion of 1+ (0.1 – 15 cm) COTS are visible and hence culled. This allows us to compute a more accurate CPUE that is comparable to what is measured in the field.

To complement the above equilibrium (static) analysis, we also used our dynamic COTS model (Morello et al., in press) to evaluate the effect of manual lethal injection on different proportions of age 1 and age 2+ COTS at different levels of coral cover. This category of models is termed “Models of Intermediate Complexity for Ecosystem assessments” (MICE) and has a tactical focus, including use as ecosystem assessment tools (Plagányi et al. 2014). MICE are context- and question-driven and limit complexity by restricting the focus to those components of the ecosystem needed to address the main effects of the management question under consideration. MICE estimate parameters through fitting to data, use statistical diagnostic tools to evaluate model performance and account for a broad range of uncertainties. These models therefore address many of the impediments to greater use of ecosystem models in strategic and particularly tactical decision-making for marine resource management and conservation.

Lastly, we use a COTS fertilisation model, parameterised with field data, to explore the relationship between COTS density and the reproductive potential of the population. Hence we examine whether there is a critical COTS density below which fertilisation fails, as this aids further in quantifying the density at which COTS remain at sub-outbreak compared with outbreak levels.

The age-size equivalence assumed throughout our work is summarised in Table 1.1 base on Pratchett (2005, 2010) and Pratchett et al. (2014).

Table 1.1 Age-size-life-stage equivalence assumed for COTS in this report and in the MICE model (Morello et al. in press), based on (2005, 2010) and Pratchett et al. (2014).

Age	Size (diameter, mm)	Stage	Age class used in report and MICE model
11+ days	0.5	newly settled juvenile	
0.5 – 6 months	1 – 10	algal feeding juvenile	age 0
0.5 – 2 years	10 – 150	coral-feeding juv. to sub-adult	age 1
>2 years	>150 - 350	coral-feeding adult	age 2+

2 Question 1. For a given level of coral cover/composition, what is the threshold level of COTS (of a given size distribution) above which coral cover will decline?

2.1 Summary and Key Conclusions

- Available data from Lizard Is. (Fisk and Power 1999) were used to fit the parameters of a preliminary hyperstable relationship between COTS removal catch-per-unit-effort (CPUE) and corresponding COTS densities (Figure 2.2)
- Drawing from a modelling and empirical analysis threshold paper currently in press, we determined the threshold of coral cover beyond which COTS are not able to survive at five different locations around Lizard Island (Table 2.2)
- The CPUE-COTS hyperstable relationship was used to convert these densities into CPUE values. On average the critical ecological threshold COTS density is 7.1 (±2.3) 2+ COTS ha^{-1} which equates to a COTS (removal) CPUE value of 0.028 (±0.01) 2+ COTS/min (Table 2.2). This is the point at which there is an abrupt decline in COTS such that the population is unable to sustain itself, and occurs at a low coral cover of approximately 14%.

2.2 Introduction

This analysis focuses on determining the relationship between COTS CPUE and COTS density and applying it to model results towards determining critical COTS density thresholds.

In order to relate COTS ecological thresholds which are measured in terms of COTS density to field-based COTS removal or observation rates, it was first necessary to determine the relationship between COTS removal catch-per-unit-effort (CPUE) and corresponding COTS densities, and estimate the parameters that drive this relationship. This exercise will allow the theoretical estimation of CPUE given a certain density of COTS or vice versa. The parameters describing the COTS CPUE – density relationship need to be obtained from field data and experiments. These experiments are currently underway by other members of the informal COTS research working group[1] and the results will be useful to improve the preliminary analyses presented here. In this report, we use existing (historic) data to preliminarily estimate the COTS CPUE – density relationship. These data were collected from a small area of Lizard Island during a previous COTS outbreak (see section 2.3.1) using methods that are at least 2.5 times less efficient than today's removal methods (J. Hoey pers. comm.). They are used here with the purpose of illustrating how this relationship can be calculated and how it can then be applied to translate model-based estimates of ecological thresholds to equivalent measures used by field practitioners.

Thus, for example, if the COTS population trajectories with different initial levels of coral are simulated using the COTS MICE model, then the CPUE-COTS relationship can be used to extrapolate CPUE values for

[1] The informal COTS research working group is a small group of researchers from CSIRO, ARC CoE, and AIMS with the aim of analysing and publishing data from the current management program and addressing important knowledge gaps to inform a longer-term Integrated Management Framework (being led by the GBRMPA).

given numbers of COTS predicted by the model under the different scenarios considered. Conversely, COTS biomass can then also be derived if CPUE is known.

Here we describe the preliminary work done to illustrate the first steps of how this could be achieved. The aim is to produce a preliminary relationship that we can use in our subsequent analyses, and also to set up a 'straw man' that can be validated or corrected as data from the field study become available. Subsequent improvements, based on further field studies, can then readily be incorporated in the modelling analyses.

2.3 Methods

2.3.1 CPUE-COTS RELATIONSHIP

The relationship between CPUE (measured as COTS removed/injected per unit time) and COTS density is unlikely to be linear as searching and handling time constraints will mean that at high COTS densities there is an upper limit to the number of COTS that can be removed/injected per unit time. Hence it is more likely that the relationship is a hyperstable one, supported also by the fact that a hyperstability relationship is the most common form of relationship used in fisheries to describe non-proportionality between CPUE and abundance in cases where CPUE remains high while abundance declines (Hilborn and Walters 1992).

The relationship between COTS removals and total COTS density was assumed to be:

$$\mathrm{CPUE} = q(N^h) \qquad \text{Eqn 2.1}$$

Where CPUE is the catch of adult COTS per unit of effort (i.e. COTS > 11cm), *q* is the catchability coefficient (the proportion of the total COTS population caught using the removal method in question), *N* is the COTS population (> 11 cm) in the water as counted by Fisk and Power (1999 – see paragraph below), and *h* is the hyperstability coefficient determining the shape of the relationship (note that *h*=1 implies a linear relationship, *h*=0 no relationship).

In order to fit the above equation to available data, we developed a model in AD Model builder (Fournier et al. 2012) and its estimation routines were used to estimate the parameters of this relationship. AD Model Builder uses quasi-Newton automatic differentiation for statistical inference (Fournier et al. 2012) and, for converged model solutions, computes Hessian-based standard error estimates to assess the precision with which the parameters are estimated. The model was run using fixed values of *h* and estimating *q*, as well as attempting to estimate both *q* and *h.*

The model was fit to removal data derived from Fisk and Power (1999). These data were collected from two small reefs around Lizard Island between October 1995 and August 1996. They comprise catch per unit effort (COTS removed·h^{-1}) and COTS density estimates (COTS·Ha^{-1}). The removal strategy was such that COTS were killed using sodium bisulphate injections and, in this particular case, each reef was visited weekly for first ten weeks and then every 2 weeks for following 20 weeks. On each visit the injection effort was a standard of 2 person hours. COTS densities were determined every four months (four times within the period) by 50x50m belt transects, before COTS were removed.

2.3.2 APPLYING THE CPUE-COTS RELATIONSHIP TO MODEL RESULTS

Using the best fit model (*h* = 0.5), the CPUE-COTS relationship was used to translate COTS biomass from different sources (e.g. model outputs or other analyses) into CPUE. This was done in two instances:

(i) For the COTS densities corresponding to the minimum threshold of coral cover below which COTS populations decline to sub-outbreak densities at five different locations around Lizard island, as illustrated in Plagányi et al. (minor revisions currently for MEPS) (corresponding to the red dots in Figure 2.1). This analysis is based on COTS and coral data reported in Pratchett (2005, 2010) which refer to COTS individuals mostly larger than 15 cm, corresponding to our 2+ age class (Table 1.1). The CPUE-COTS relationship described above was used to convert these densities into CPUE values.

(ii) For the COTS abundance predictions generated by the COTS MICE model outlined in Morello et al. (in press). To do this, the COTS predictions (COTS·manta tow^{-1} from AIMS LTMP) were converted to densities (COTS·Ha^{-1}) assuming each 2 min manta tow to cover an area of approximately 0.15 Ha (Ayling and Ayling 1992, Moran and De'ath 1992). This preliminary estimate may be revised in consultation with the project team.

2.4 Results and Discussion

2.4.1 CPUE-COTS RELATIONSHIP

The catchability parameter *q* of the CPUE-COTS relationships was estimated with good precision (Table 2.1). This only applied to values of *h* between 0.5 and 1.0; at values of *h* lower than 0.5, the estimated values of *q* were impossible (> 1.0). The CPUE trajectories calculated using the parameters summarised in Table 2.1 are illustrated in Figure 2.2 which shows that as *h* increases, the relationship between CPUE and COTS biomass progressively tends towards linearity (*h* = 1). The likelihoods computed for each alternative model measure the probability of the data given the parameter estimates, and therefore comparisons of likelihoods can be used to select the model which fits the data best statistically. The best model fit and hence relationship is described by *h*=0.5 (denoted with * in Table 2.1, Figure 2.2).

2.4.2 APPLYING THE CPUE-COTS RELATIONSHIP TO MODEL RESULTS

The CPUEs derived from the COTS densities corresponding to the coral threshold levels beyond which COTS populations are not able to sustain themselves, as reported in Plagányi et al. (in press) are summarised for five different locations around Lizard Island in Table 2.2. They were also overlaid to the CPUE-COTS relationship (*h* = 0.5) in Figure 2.3. On average the critical ecological threshold COTS density is 7.1 (±2.3) 2+ COTS ha^{-1} which equates to a COTS (removal) CPUE value of 0.028 (±0.01) 2+ COTS/min (Table 2.2). This is the point at which there is an abrupt decline in COTS such that the population is unable to sustain itself, and occurs at a low coral cover of approximately 14%. In essence, if there is no control but COTS are at densities of 7.1 ha-^{1} and there coral cover is below 14%, the COTS population will collapse because of starvation.

The CPUE values corresponding to the COTS abundance predictions generated by the Morello et al. (in press) MICE model are illustrated in Figure 2.4 and overlaid with the CPUE threshold determined in Table 2.2 (1.70 2+ COTs hr^{-1}).

2.4.3 COMPARABILITY OF THRESHOLD ESTIMATES

One of the main aims of this work is to show how existing data sets can be used in combination with numerical modelling approaches to derive population thresholds for use in management applications. Due to the nature of the historical data sets, which were not collected for this purpose, as well as constraints of time, differing data sets have had to be used for various steps in this process. For this reason these threshold estimates must be considered preliminary. While this is unavoidable at this time, there exists the opportunity to ensure that ongoing data collections capture the data necessary for continually improving these threshold estimates.

Table 2.1 Estimates of *q* at different fixed values of *h* to different values, including the asymptotic standard errors (SD), coefficients of variation (CV) and likelihood values (calculated as the sum of squares). * denotes the best relationship.

h	q	SD	CV	Likelihood
0.5	0.669	0.011	0.016	322.87*
0.6	0.374	0.006	0.016	346.35
0.7	0.206	0.003	0.016	383.15
0.8	0.112	0.002	0.016	428.26
0.9	0.061	0.001	0.016	477.61
1.0	0.033	0.001	0.017	528.13

Table 2.2 COTS densities corresponding to the threshold of coral cover below which COTS populations decline to sub-outbreak densities , as illustrated in Plagányi et al. (in press) and associated values of CPUE according to the CPUE-COTS relationship where *h* = 0.5, for five areas around Lizard Island in the GBR

Reef	Coral threshold (% cover)	COTS threshold (2+ COTS Ha^{-1})	CPUE (2+ COTS hr^{-1})	CPUE (2+ COTS min^{-1})
North reef	13	3.0	1.16	0.019
Lizard Head	13	4.0	1.34	0.022
South island	18	4.5	1.42	0.024
Casuarina	16	8.3	1.92	0.032
Corner Beach	10	15.5	2.64	0.044
Average	14	7.1	1.70	0.028

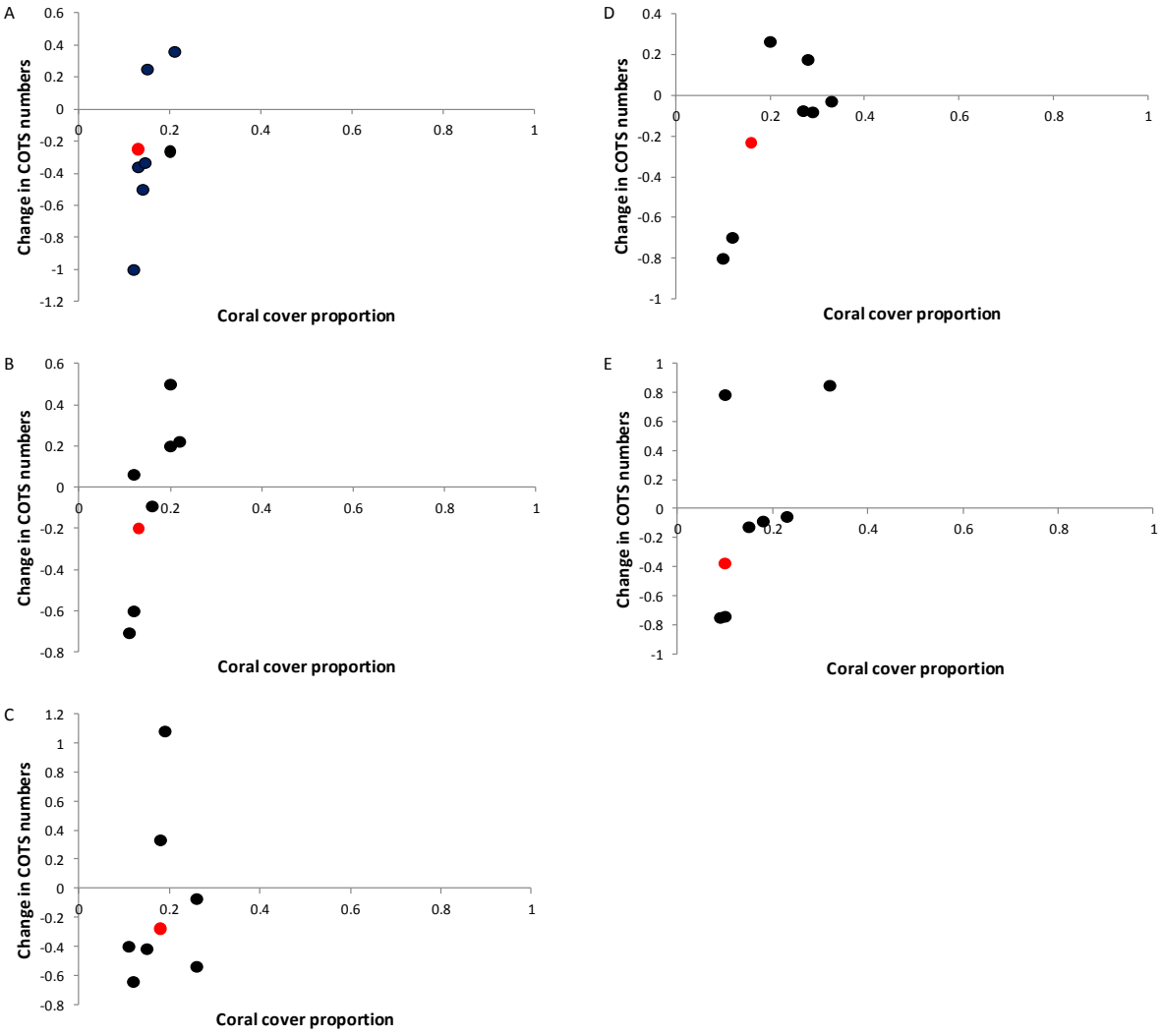

Figure 2.1 Observed rates of change in COTS and corals as a function of the relative depletion of corals: crown-of-thorns starfish (COTS) which prey on fast-growing coral at five different locations on Lizard Island (Great Barrier Reef) (data from Pratchett 2005, 2010). (A) North Reef, (B) Lizard Head, (C) South Island, (D) Casuarina, (E) Corner Beach. Relative depletion of COTS was calculated as the current coral abundance relative to the maximum observed value (used as a proxy for pristine abundance). Red dots indicate the points that were selected as threshold values, i.e. where the derivative is greatest. Figure modified from Plagányi et al. (in press).

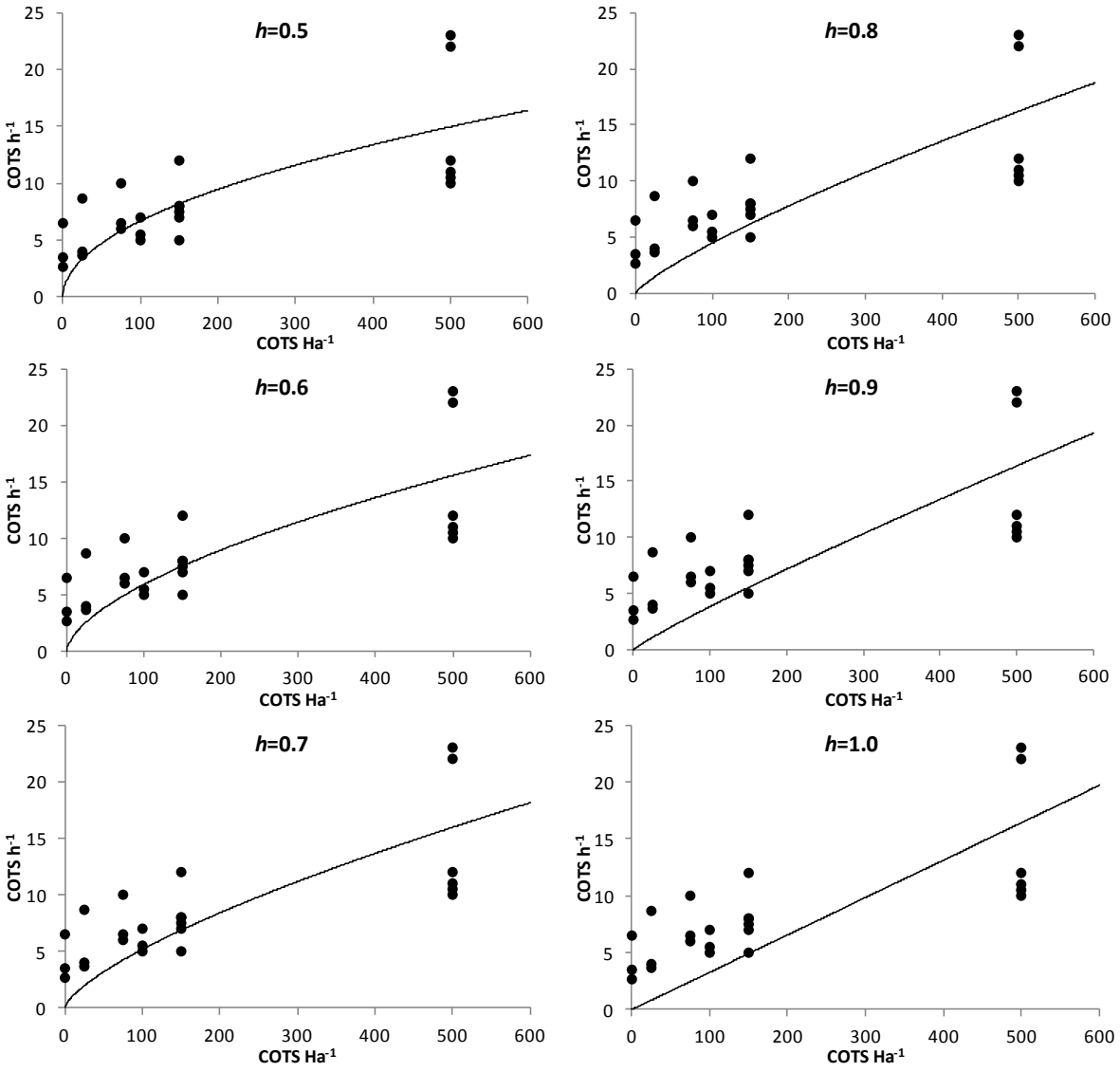

Figure 2.2 Catch per unit effort (COTS·h^{-1}) against COTS biomass (COTS·Ha^{-1}) for different values of *h*

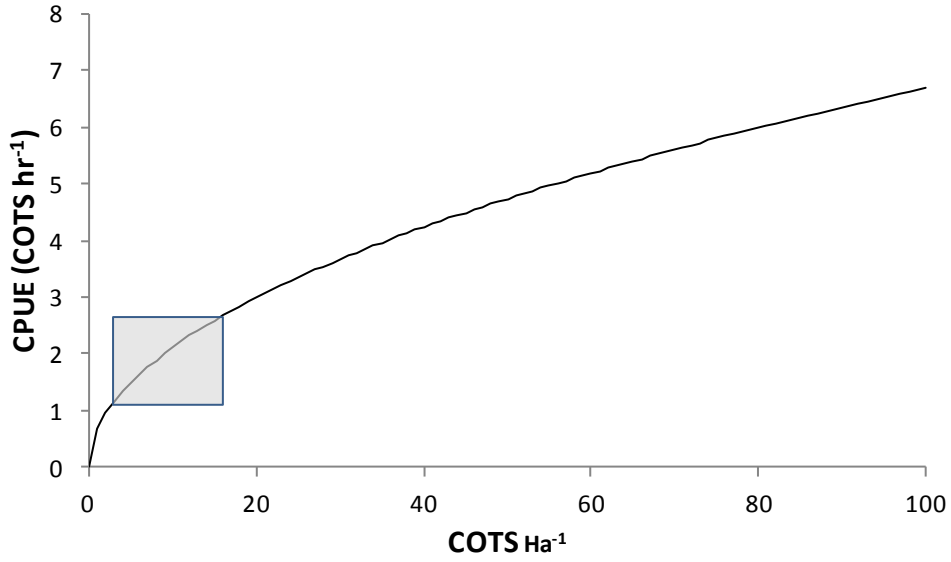

Figure 2.3 The results summarised in Table 2 (shaded box) overlaid to the CPUE-COTS relationship based on *h* = 0.5.

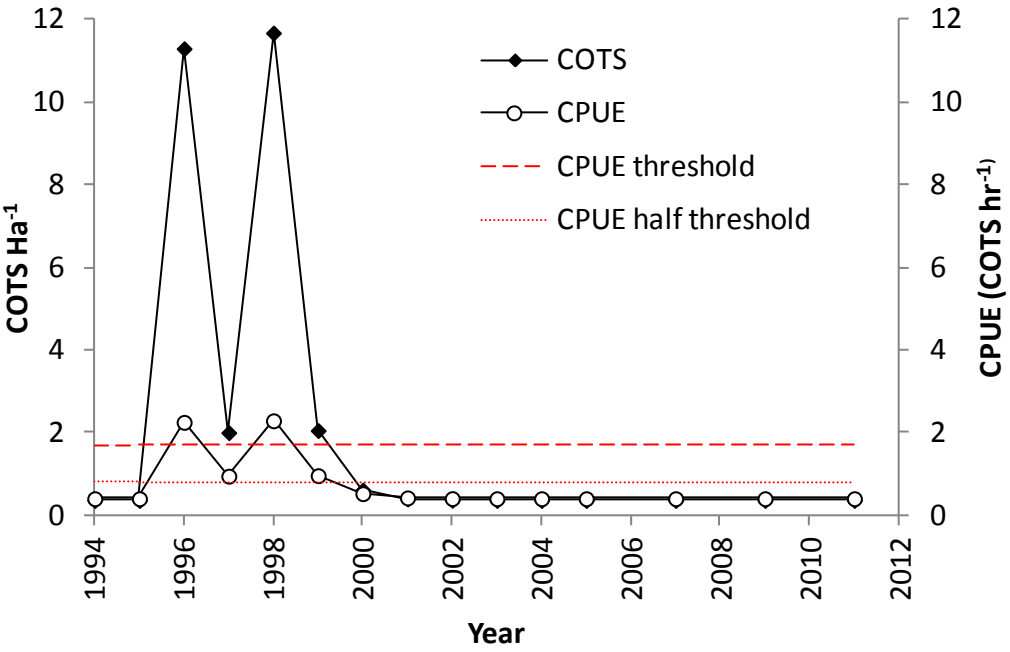

Figure 2.4 2+ COTS densities predicted by the COTS MICE model (Morello et al. in press) and corresponding CPUE values according to the CPUE-COTS relationship where *h* = 0.5. The dashed lines show the COTS CPUE average threshold value from Table 2.2, as well as half this value.

3 Question 2A: What is the threshold level of coral cover and coral diversity that needs to remain/be protected to enable the reef to recover.

3.1 Summary and Key Conclusions

- The numbers of COTS measured per tow are converted to units of hectares using the relationship: (COTS ha^{-1}) = (cots/tow)/0.15, based on Ayling and Ayling (1992) and Moran and De'ath (1992)
- The COTS densities are presented as the number of age 2+ COTS ha^{-1} because this is the measurement that most readily relates to CPUE measures
- The Morello et al. (in press) model equations and best fit parameter estimates are used to solve for the number of COTS that keeps fast-growing coral in equilibrium at different coral cover levels (Figure 3.1A, Table 3.4).
- For fast-growing coral, there are trade-offs between the rate of growth of coral and the removal through COTS predation. The model steady state analysis suggests that if coral cover is high, then the same number of COTS will have less impact on the system than for lower levels of coral cover (Figure 3.1A). Hence more COTS are needed to reduce the coral cover below equilibrium at higher coral cover levels: for example, if the coral cover is 80%, then the model suggests that as many as 20 COTS ha^{-1} (2+ animals) can be sustained without causing a further decline in the (fast-growing) coral cover, compared with 9 COTS ha^{-1} when the coral cover is 40%, and 5 COTS ha^{-1} when the coral cover is 20%.
- The number of COTS that keep slow-growing coral in equilibrium is also solved for a range of different steady state fast-growing coral depletion levels. Results suggest that if the fast growing corals are depleted, the more rapidly COTS will switch to feeding on slow growing massive corals and hence relatively fewer COTS are needed to reduce the cover of massive corals below equilibrium level. Much lower numbers of COTS are predicted to have an impact on massive corals (compared with fast growing corals) because of the slower growth rate of these species.
- Model results are compared with the outbreak threshold (10 COTS Ha^{-1}) defined by Keesing and Lucas (1992) for coral cover in the range 20% to 50%, and there is excellent agreement between the results over this range of coral cover (Figure 3.1). Our model suggests outbreak thresholds are in the range 5 – 12 COTS ha^{-1}, depending on coral cover.
- The 2+ and total (1+ and 2+ combined) COTS densities are converted to preliminary CPUE rates. If the coral cover is 20-40%, then the model suggests that the equilibrium COTS CPUE for 2+ and total numbers respectively is 0.026-0.034 COTS/min and 0.096-0.127 COTS/min (Table 3.4), i.e. this is the level of COTS abundance below which coral growth exceeds COTS grazing pressure.
- Using the management program removal size structure data to compute an average size and age structure, and the natural mortality of COTS estimated by Morello et al. (in press), we calculate the sightability of age 1 (<15 cm) COTS at 19%; selectivity of age 2+ COTS was assumed to be 100%.
- We used this sightability to compute revised CPUE with units of (age 2+ & 19% of 1+ COTS) min^{-1}, which is considered the measure that is most directly comparable to field CPUE. We find that for coral cover in the range 20-40%, the COTS CPUE should be maintained below approximately 0.05-0.06 COTS/min to keep the coral cover stable at its current level. This compares well with the current management rules being implemented as follows:

  Coral cover over 40% - keep CPUE <=0.1 COTS/min (this study suggests 0.07-0.09 COTS/min)

  Coral cover approaching 20%, keep CPUE <=0.05 COTS/min (this study suggests 0.04 COTS/min)

3.2 Introduction

This analysis focuses on estimating the point at which the net growth rate in coral cover is zero.

The growth in overall cover of both fast-growing and slow-growing corals is negatively affected by the consumption by COTS. The aim of this analysis is to determine at what COTS density the net growth of coral becomes zero i.e. coral stabilises at a level. The relationship will change depending on the starting level of coral depletion (measured as proportion of coral cover). Here we explore first the predictions based on the existing COTS model of Morello et al. (in press), which is here summarised in Table 3.1, Table 3.2 and Table 3.3. Next we explore obtaining this information based on empirical information. Finally, we utilise and cross-compare results with data from GBRMPA's Eye on the Reef database (which includes COTS management cull data and Field Management Program surveillance data).

In our model two groups of corals are modelled: fast-growing coral (*Acropora* spp.), and massive slow-growing coral (e.g. Faviidae, *Porites* spp. etc.) (Table 3.1, Table 3.2). COTS prefer the fast-growing coral species and switch to consuming massive corals only at high densities or when fast-growing corals have been depleted (Birkeland & Lucas 1990). In the model, COTS therefore start consuming fast-growing coral and switch to slow-growing coral only when the density of fast-growing coral declines substantially (Table 3.1, Table 3.2).

3.3 Methods

3.3.1 COTS-CORAL MODEL EQUATIONS

The coral equation from Table 3.1can be rearranged and solved for the case of zero change in coral as follows:

$$r^f C_y^f (1-C_y^f / K^f) = (1-\rho_y) \frac{p_1^f (N_{y,1}+N_{y,2}) C_y^f}{1+\exp\left(-(N_{y,1}+N_{y,2})/p_2^f\right)} \quad \text{Eqn 3.1}$$

And hence substituting for p_y, this simplifies to:

$$\frac{r^f}{p_1^f} \frac{(1-C_y^f / K^f)}{\exp(-5C_y^f / K^f)} = \frac{(N_{y,1}+N_{y,2})}{1+\exp\left(-(N_{y,1}+N_{y,2})/p_2^f\right)} \quad \text{Eqn 3.2}$$

For different values of coral depletion (C/K), a Newton-Raphson root-finding method is then used to solve for the number of COTS aged one year and older $(N_{y,1}+N_{y,2})$ that keeps the coral in equilibrium at a pre-specified level. The total number of COTS is $N_y = N_{y,1}+N_{y,2}$ and this can be further separated into the number of 1 year old and 2+ animals using the relation:

$$N_{y,2} = \frac{N_y}{(1+e^M)} \quad \text{Eqn 3.3}$$

$$N_{y,1} = N_y - N_{y,2} \quad \text{Eqn 3.4}$$

Lastly, the model numbers of COTS measured per tow, can be converted to units of hectares using the relation:

$$(\text{Cots/Ha}) = (\text{Cots/tow}) / 0.15 \qquad \text{Eqn 3.5}$$

The COTS densities in our initial analyses are presented as the number of 2+ COTS ha^{-1} but this is subsequently revised to obtain a measure that most readily relates to CPUE measures.

Similarly, for the slow-growing coral, the following equation can be used to solve for the number of COTS that keeps the coral in equilibrium, except that this is simultaneously a function of the depletion level of the fast-growing coral (because of the swap function – Equation 7 in Table 3.1):

$$\frac{r^m}{p_1^m}\frac{(1-C_y^m / K^m)}{(1+\exp(-5C_y^f / K^f))} = \frac{(N_{y,1}+N_{y,2})}{1+\exp\left(-(N_{y,1}+N_{y,2}) / p_2^m\right)} \qquad \text{Eqn 3.6}$$

The number of COTS that keep slow-growing coral in equilibrium is therefore solved for a range of different steady state fast-growing coral depletion levels.

The preliminary relationship obtained between COTS removals and COTS density (see section 2) was used to roughly estimate equilibrium COTS CPUE values:

$$\text{CPUE} = 0.669(N^{0.5}) \qquad \text{Eqn 3.7}$$

3.3.2 COMPARING MODEL RESULTS AND MANAGEMENT PROGRAM DATA

The management program cull data includes specification of size classes as follows:

- <15cm (age 1)
- 15-25cm (age 2+)
- 25-40cm (age 2+)
- >40cm (age 2+)

These sizes correspond to the age classes in Table 1.1 which are based on Pratchett (2005, 2010) and Pratchett et al. (2014). Thus, as a preliminary age-length split, we assume the categories <15cm to COTS that are less than two years old, whereas the three larger categories correspond to age 2+ COTS. Noting that small COTS individuals can be cryptic, following advice from AMPTO it was determined that COTS less than 10cm were more difficult to find. Given the lower size category extends to <15cm we would like to know the relative proportions of 1+ and 2+ animals removed as part of the management program. As a preliminary data analysis, we summed all the data from all reefs in the removals spreadsheet and computed the average size (and age) distribution as shown in Figure 3.2A and Table 3.5. The proportions by age in the two age categories (<2yrs; > 2yrs) are approximately equally divided (Table 3.5). Given that the divers likely remove all 2+ COTS (based on advice from AMPTO), we assume full selectivity of that age class, but we don't know what proportion of the 1+ animals they see and remove so need a selectivity proportion for this age class, which we denote by *s*.

Based on the natural mortality estimate in our model (see Eqn. 3.3 above), we can predict what the average COTS age distribution should be, and this yields a relative proportion of 1+ compared to 2+ animals of 78%:22% (Table 3.5). Hence this substantiates that as expected, divers will "miss" some age 1+ animals in their removals, and we derived preliminary estimates of the selectivity of the 1 animals as *s*= 19% (based on the observed: expected proportion in the first age class).

The next step is to sum our model 2+ numbers plus 19% of the 1+ numbers to yield a total (labelled 2+ & 19% of 1+ COTS) number of COTS which is the number that is predicted to be most comparable to field effort. This new COTS total is then used to compute a revised CPUE (using Eqn. 3.7 hyperstability relationship) with units of (age 2+ & 19% of 1+ COTS)/min which is therefore the measure that is most directly comparable to field CPUE measures (i.e. it accounts for the size distribution of animals removed in the field).

3.4 Results

3.4.1 COTS-EQUILIBRIUM CORAL RELATIONSHIP

The point at which COTS consumption of coral outstrips coral growth is key to the ecology and management of the relationship between COTS on coral reefs. Model results are compared with the outbreak threshold (10 COTS Ha^{-1}) defined by Keesing and Lucas (1992) for cover of fast growing coral (Coralf) in the range 20% to 50%, and there is excellent agreement between the results across this range of coral cover. The number of COTS required to cause net change in coral cover declines near mimimum and maximum values because coral cover is constrained by the of the 0 and 100% bounds. In this context coral assemblages with approximately 80% cover of fast growing coral show the greatest resistance to COTS impact on net cover (Figure 3.1). Much lower densities of COTS are required in order to produce a negative impact on slow growing coral populations (Figure 3.1), because they grow much more slowly, and net cover declines linearly with increasing COTS density, in contrast to the relationship for fast growing corals.

Figure 3.1 shows the number of COTS (2+ animals/ha) that restrict (A) the fast-growing and (B) the slow-growing coral cover at a zero growth rate level for coral cover at a range of levels as shown. Values for COTS at levels below the curves are sub-outbreak densities, that is the rate of consumption of corals by COTS is below the net growth rate of the coral assemblages.

The number of COTS is shown in units of both numbers of large age 2+ COTS ha^{-1} as well as the total number of 1+ and 2+ COTS ha^{-1} (Table 3.4). The 2+ and total COTS densities are converted to preliminary CPUE rates, providing a basis for enabling management programs to make operational estimates of COTS CPUE target levels at reefs with a range of coral cover

3.4.2 COMPARING MODEL RESULTS AND AMPTO DATA

The revised CPUE (using Eqn. 3.7 hyperstability relationship) with units of (age 2+ & 19% of 1+ COTS)/min which is considered the measure that is most directly comparable to field CPUE measures (i.e. it accounts for the size distribution of animals removed in the field) is shown in Table 3.5. These revised measures are used to produce a plot of the COTS CPUE (comparable to field CPUE estimates) that restricts the fast-growing coral cover at a zero growth rate level for coral cover across a range of levels as shown in Figure 3.3 (with values shown in Table 3.7).

For coral cover in the range 20-40%, these preliminary results suggest that the COTS CPUE should be below approximately 0.05-0.06 COTS/min to maintain coral cover at its current level and promote recovery. Figure 3.3 also shows the average (+STD) coral cover from the reefs that form part of the COTS management program was 35% (Table 3.6), within the range described above.

3.5 Discussion

For fast-growing coral, there is a point at which the balance between the rate of growth of coral and the removal through grazing by COTS moves from net growth to net decline. The model steady state analysis suggests that if coral cover is higher, then the same number of COTS will have less impact on the system than for lower levels of coral cover (Figure 3.1A). Hence more COTS are needed to prevent net growth in cover at higher coral cover levels: for example, if the coral cover is 80%, then the model suggests that as

many as 20 COTS ha^{-1} (2+ animals) could be present on a reef without causing a further decline in the coral cover, compared with 5 COTS ha^{-1} when the coral cover is 20%. At high levels of coral cover it may be desirable to reduce COTS densities well below the cover-specific outbreak level, particularly where this may be at or above threshold levels of fertilization success or zygote production. This may have the benefit of inhibiting secondary outbreak and would need to be a factor in prioritization and triage around a regional COTS management program.

In order to try and validate results using empirical information, we compared our model results with the outbreak threshold (10 COTS Ha^{-1}) defined by Keesing and Lucas (1992) which was derived based on data for reefs having a coral cover ranging between 20% and 50% (Figure 3.1A). This cover also aligns closely with the average coral cover recorded on reefs as part of the COTS management program. Our model results compare well with these empirical estimates, suggesting outbreak thresholds are in the range 5 – 12 COTS ha^{-1} (Table 3.4).

The shape of the curve in Figure 3.1 is similar to a sustainable yield curve as classically used in fisheries management, and is shifted to the right because of the high growth rate of fast-growing coral. The sensitivity to alternative assumed coral growth rates can readily be investigated. This contrasts with the shape estimated for slow-growing coral, because the latter has a much slower rate of growth. The COTS are assumed to switch to feeding on slow-growing corals once the fast-growing corals become heavily depleted (Moran 1986). Figure 3.1B suggests that if the fast-growing coral are more heavily depleted, the COTS will switch more rapidly to feeding on slow-growing coral and hence relatively fewer COTS are needed to maintain the slow-growing coral at a pre-specified depletion level. Sensitivity to alternative growth rates of slow-growing coral can similarly be readily investigated. Alternative growth scenarios for both fast and slow growing corals might include varying rates of impacts such as cyclone damage and coral bleaching.

The number of COTS that keeps fast-growing coral in equilibrium is shown in units of both numbers of large age 2+ COTS ha^{-1} as well as the total number of 1+ and 2+ COTS ha^{-1}. A diver searching underwater will mostly see (and subsequently record or cull) the large 2+ COTS because the younger (smaller) animals are cryptic, but some of the 1+ animals will undoubtedly be sighted too, and hence the results are shown also in terms of total 1+ and 2+ animals. Additional analyses were then done to clarify the length-age relationship to further refine these estimates i.e. to calculate more exactly what proportion of the 1+ COTS are typically sighted by a diver.

The 2+ and total COTS densities are converted to preliminary CPUE rates. If the coral cover is 20-40%, then the model suggests that the equilibrium COTS CPUE (2+ animals) is approximately 0.026-0.034 COTS/min or COTS CPUE (total animals) is approximately 0.096-0.127 COTS/min (Table 3.4).

Next we used the size structure data to compute an average size structure, in turn roughly converted to an age distribution (Figure 3.2). This conversion can be refined as more data and information become available. We compared this distribution to the model-derived expected distribution of animals actually present in the field (assuming stable growth), and in this way estimated that the selectivity of the 1+ animals (those we classified as younger than 2 years) is 19% (Table 3.5), i.e. on average, we estimate that divers find and remove 19% of these younger animals. The selectivity parameter could be estimated in a more sophisticated modelling process, but that is beyond the scope of this current study.

Next we computed the revised CPUE with units of (age 2+ & 19% of 1+ COTS)/min, which is considered the measure that is most directly comparable to field CPUE measures (i.e. it accounts for the size distribution of animals removed in the field). Finally we plot the COTS CPUE (comparable to field CPUE estimates) that restricts the fast-growing coral cover at a zero growth rate level for coral cover across a range of levels as shown in Figure 3.3. For coral cover in the range 20-40%, these preliminary results suggest that the COTS CPUE should be maintained below approximately 0.05-0.06 COTS/min to keep the coral cover stable at its current level. The average (+STD) coral cover is 35% ($\pm$17%) with range 3-88% (Table 3.6) suggesting that on average CPUE target rates should be less than 0.06 COTS/min and for low coral cover, CPUE target rates should be lower, down to around 0.04 COTS/min (Table 3.7).

This compares well with the current management rules being implemented as follows:

Coral cover over 40% - keep CPUE <=0.1 COTS/min (this study suggests 0.07-0.09 COTS/min)

Coral cover approaching 20%, keep CPUE <=0.05 COTS/min (this study suggests 0.04 COTS/min)

Note also that the finding from this study that the sub-outbreak threshold density of COTS (and hence the CPUE) is reduced at lower coral cover (Figure 3.1A, Figure 3.3), provides scientific support for the current management approach which increases the number of COTS to be removed when coral cover is below rather than above 40%.

Note also that these results are preliminary only at this stage and may be refined as further data and information become available.

Table 3.1 Model equations for key groups

Functional group	Equation	No.
Basic Population Dynamics		
COTS		
Age 0	$N_{y+1,0} = R_{y+1} + I\, e^{\eta_{y+1}}$; $R_y = \frac{4hR_0\, N_{y,2+}/K^{Cots}}{(1-h)+(5h-1)N_{y,2+}/K^{Cots}} e^{\varepsilon_y}$	1a
Age 1	$N_{y+1,1} = N_{y,0}\, e^{-f(C_y^f)M^{Cots}} - Q_{y,0}^{Cots}$	1b[1]
Age 2+	$N_{y+1,2+} = (N_{y,1} + N_{y,2+})e^{-f(C_y^f)M^{Cots}} - Q_{y,2+}^{Cots} - H_y^{Cots}(\Phi_1^{Cots} N_{y,1} + N_{y,2+})$	1c[1]
Fast-growing coral	$C_{y+1}^f = C_y^f + r^f C_y^f (1 - C_y^f / K^f) - Q_y^f$	2
Slow-growing coral	$C_{y+1}^m = C_y^m + r^m C_y^m (1 - C_y^m / K^m) - Q_y^m$	3
Large fish predators	$P_{y+1} = P_y g(C_y^f) S^P (1 - F^P) + P_{y-T^P+1} R^P g(C_{y-T^P+1}^f)(S^P)^{T^P}$	4[2]
Trophodynamic Interaction Terms		
Predation on COTS		
Age 0	$Q_{y,0}^{Cots} = F^B N_{y,0} \bar{B}$	5a
Age 2+	$Q_{y,2+}^{Cots} = \frac{(N_c)^\mu}{(N_{y,2+})^\mu + (N_c)^\mu} \frac{p_1^{Cots} N_{y,2+} P_y}{1+\exp\left(-N_{y,2+}/p_2^{Cots}\right)}$	5b
COTS Predation on coral		
Fast-growing	$Q_y^f = (1-\rho_y) \frac{p_1^f (N_{y,1}+N_{y,2}) C_y^f}{1+\exp\left(-(N_{y,1}+N_{y,2})/p_2^f\right)}$	6a
Slow-growing	$Q_y^m = \rho_y \frac{p_1^m (N_{y,1}+N_{y,2}) C_y^m}{1+\exp\left(-(N_{y,1}+N_{y,2})/p_2^m\right)}$	6b
Swap function	$\rho_y = \left(1+\exp(-5C_y^f / K^f\right)$	7
Coral abundance on COTS mortality	$f(C_y^f) = 1 - \tilde{p} \frac{C_y^f}{1+C_y^f}$	8
Coral abundance on predator survival	$g(C_y^f) = 1 - \tilde{\tilde{p}} \frac{C_y^f}{1+C_y^f}$	9

Table 3.2 Description of the variables of the model.

Functional group	Description
COTS	
$N_{y,a}$	Number of COTS of age *a* at the start of (calendar) year *y*
R_y	Self recruitment during year *y*
$Q_{y,a}^{Cots}$	Number of COTS of age *a* consumed by predators during year *y* (age-0 animals by benthic invertebrates; age-2+ animals by large fish predators)
M_a	Natural mortality at age *a*
Fast-growing coral	
C_y^f	Biomass of fast-growing coral at the start of year *y* [3]
Q_y^f	Biomass of fast-growth coral consumed by COTS during year *y*
Slow-growing coral	
C_y^m	Biomass of slow-growing coral at the start of year *y*[3]
Q_y^m	Biomass of slow-growth coral consumed by COTS during year *y*
Large fish predators	
P_y	Number of large fish predators at the start of year *y*

Table 3.3 Model input parameters

Parameter	Description	Value	Rationale / Notes
COTS			
$COTS_{init}$	Initial number of 2+ COTS	Estimated	The numbers of age 1+ and age 0 COTS are computed by multiplying the value of $COTS_{init}$ by $e^{M^{Cots}}$ and $e^{2M^{Cots}}$ respectively.
ε_y	Stock-recruitment residual for year *y*	0 for all years except 1996	The value for 1996 is estimated
I	Median background immigration	1	
η_y	Immigration residual for year *y*	0 for all years except 1994	The value for 1994 is estimated
h	Stock-recruitment steepness	1	Implies that self-recruitment is constant in expectation
R_0	Unfished recruitment	1	
K^{Cots}	Carrying capacity	N/A	Does not impact the dynamics given the assumed value for *h*
M^{Cots}	Natural mortality	Estimated	
p_1^{Cots}	Predation effect of large fish on COTS	0	Non-zero values are considered in the projections
p_2^{Cots}	Predation effect of large fish on COTS	50	Pre-specified as it is correlated with p_1^{Cots}
$\tilde{p}$	Effect of fast coral on COTS mortality	Estimated	
N_c	Saturation parameter	0.5	Pre-specified after initial model tuning
μ	Saturation parameter	5	Set so that there is a rapid switch between fast-growing and slow-growing coral when coral biomass drops below N_c
ω	Mortality estimated by fitting the model	2.560yr^{-1}	Natural mortality estimated by the base case model
λ	Parameter controlling the difference between mortality rates of younger and older animals	0.1, 0.2, 0.3, estimated	Parameter λ can be either estimated or fixed to a constant
Fast-growing coral			
C_{init}^f	Initial biomass	Set to K^f	
r^f	Intrinsic rate of growth	0.5 yr^{-1}	Pre-specified after initial model tuning
K^f	Carrying capacity	2500	Arbitrary*
p_1^f	Effect of COTS on fast-growing coral	Estimated	
p_2^f	Effect of COTS on fast-growing coral	10	Pre-specified as it is correlated with p_1^f
Slow-growing coral			
C_{init}^m	Initial biomass	Set to K^m	
r^m	Intrinsic rate of growth	0.1 yr^{-1}	5-fold lower than for fast-growing coral
K^m	Carrying capacity	500	Arbitrary*
p_1^m	Effect of COTS on slow-growing coral	Estimated	
p_2^m	Effect of COTS on slow-growing coral	8	Pre-specified as it is correlated with p_1^m

Table 3.4 Summary of results showing the number of COTS that keep fast-growing coral in equilibrium at different coral cover levels as shown in Figure 3.1. The number of COTS is shown in units of both numbers of large age 2+ COTS ha^{-1} as well as the total number of 1 and 2+ COTS ha^{-1}. The 2+ and total COTS densities are converted to preliminary CPUE rates.

Fast-growing coral cover	2+COTS (no./ha)	CPUE (2+cots/hr)	CPUE (2+ cots/min)	Total COTS (no./ha)	CPUE (total cots/min)
0	2.9	1.133	0.019	40.0	0.071
0.05	3.4	1.229	0.020	47.1	0.076
0.1	4.0	1.330	0.022	55.1	0.083
0.15	4.6	1.436	0.024	64.2	0.089
0.2	5.3	1.547	0.026	74.5	0.096
0.25	6.2	1.664	0.028	86.2	0.104
0.3	7.1	1.786	0.030	99.3	0.111
0.35	8.2	1.914	0.032	114.1	0.119
0.4	9.4	2.049	0.034	130.7	0.127
0.45	10.7	2.189	0.036	149.2	0.136
0.5	12.2	2.335	0.039	169.7	0.145
0.55	13.8	2.484	0.041	192.1	0.155
0.6	15.5	2.632	0.044	215.7	0.164
0.65	17.2	2.774	0.046	239.7	0.173
0.7	18.8	2.899	0.048	261.7	0.180
0.75	20.0	2.993	0.050	278.9	0.186
0.8	20.5	3.031	0.051	286.0	0.189
0.85	19.8	2.978	0.050	276.1	0.185
0.9	17.2	2.771	0.046	239.0	0.172
0.95	11.7	2.284	0.038	162.4	0.142
1	0.0	0.025	0.000	0.0	0.002

Table 3.5 Summary of the average size structure of COTS across all reefs from the COTS management program, as well as preliminary age-length split. Comparison with model-predicted expected proportion in the two age classes is used to deduce what proportion of the younger animals are visible and removed during the management program dives.

Age	**Age < 2 years**	**Age > 2 years**		
Size category	**<15cm**	**15-25 cm**	**25-40 cm**	**>40cm**
Proportion in size category	0.144	0.360	0.341	0.155
Proportion in age class category (management program)	0.144	0.856		
Expected proportion in population (MODEL)	0.780	0.224		

Table 3.6 Summary of the average (together with associated statistics) coral cover percentage recorded as part of the COTS management program from all reefs. The average and STD values are used for comparison in Figure 3.3.

	Average coral cover	**STD**
Average	35%	17%
Minimum cover	3%	
Maximum cover	88%	
Median	33%	

Table 3.7 Summary of final results showing the number of COTS and corresponding CPUE that keep fast-growing coral in equilibrium at different coral cover levels as shown in Figure 3.1. The number of COTS is shown in units of the total number of age 2+ and 19% of age 1+ (<15 cm) COTS ha^{-1}. The COTS densities are converted to preliminary CPUE rates, shown as the number per minute and per hour, in units that have been matched as closely as possible to that recorded in the recent field surveys.

Fast-growing coral cover	COTS number per ha of 2+ animals and 19% of 1+ animals	CPUE (2+&19% of 1+ cots/min)	CPUE (2+&19% of 1+ cots/hr); units in COTS per hour
0	9.9	0.04	2.11
0.05	11.7	0.04	2.29
0.1	13.7	0.04	2.47
0.15	15.9	0.04	2.67
0.2	18.5	0.05	2.88
0.25	21.4	0.05	3.09
0.3	24.6	0.06	3.32
0.35	28.3	0.06	3.56
0.4	32.4	0.06	3.81
0.45	37.0	0.07	4.07
0.5	42.1	0.07	4.34
0.55	47.7	0.08	4.62
0.6	53.5	0.08	4.89
0.65	59.5	0.09	5.16
0.7	64.9	0.09	5.39
0.75	69.2	0.09	5.56
0.8	71.0	0.09	5.64
0.85	68.5	0.09	5.54
0.9	59.3	0.09	5.15
0.95	40.3	0.07	4.25
1	0.0	0.00	0.05

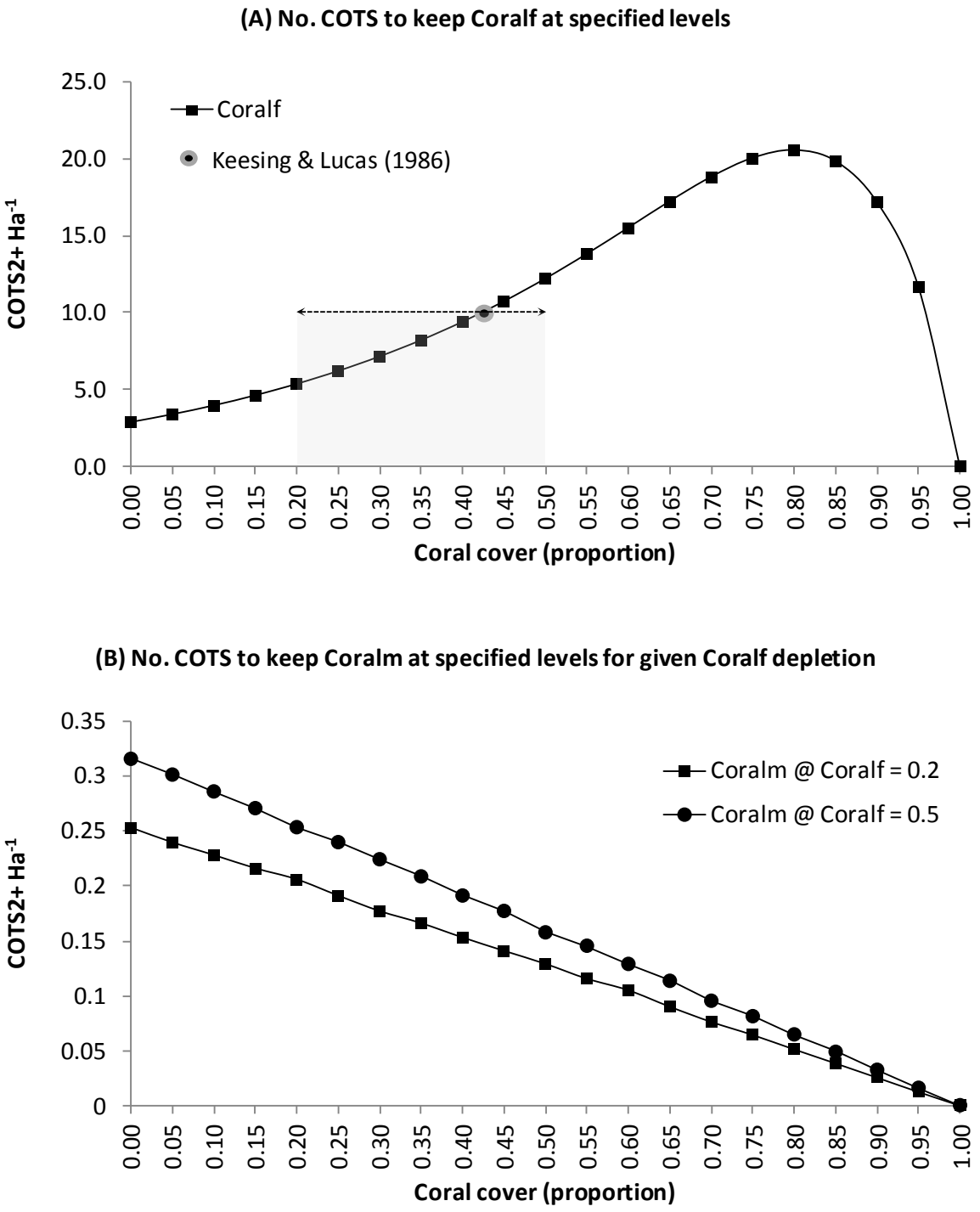

Figure 3.1 COTS density (2+ COTS·ha^{-1}) that results in (A) fast-growing coral with an indication of the outbreak threshold (10 COTS ha^{-1}) defined by Keesing and Lucas (1992) for coral cover of 20% to 50% and (B) slow-growing coral stabilising at the level as shown.

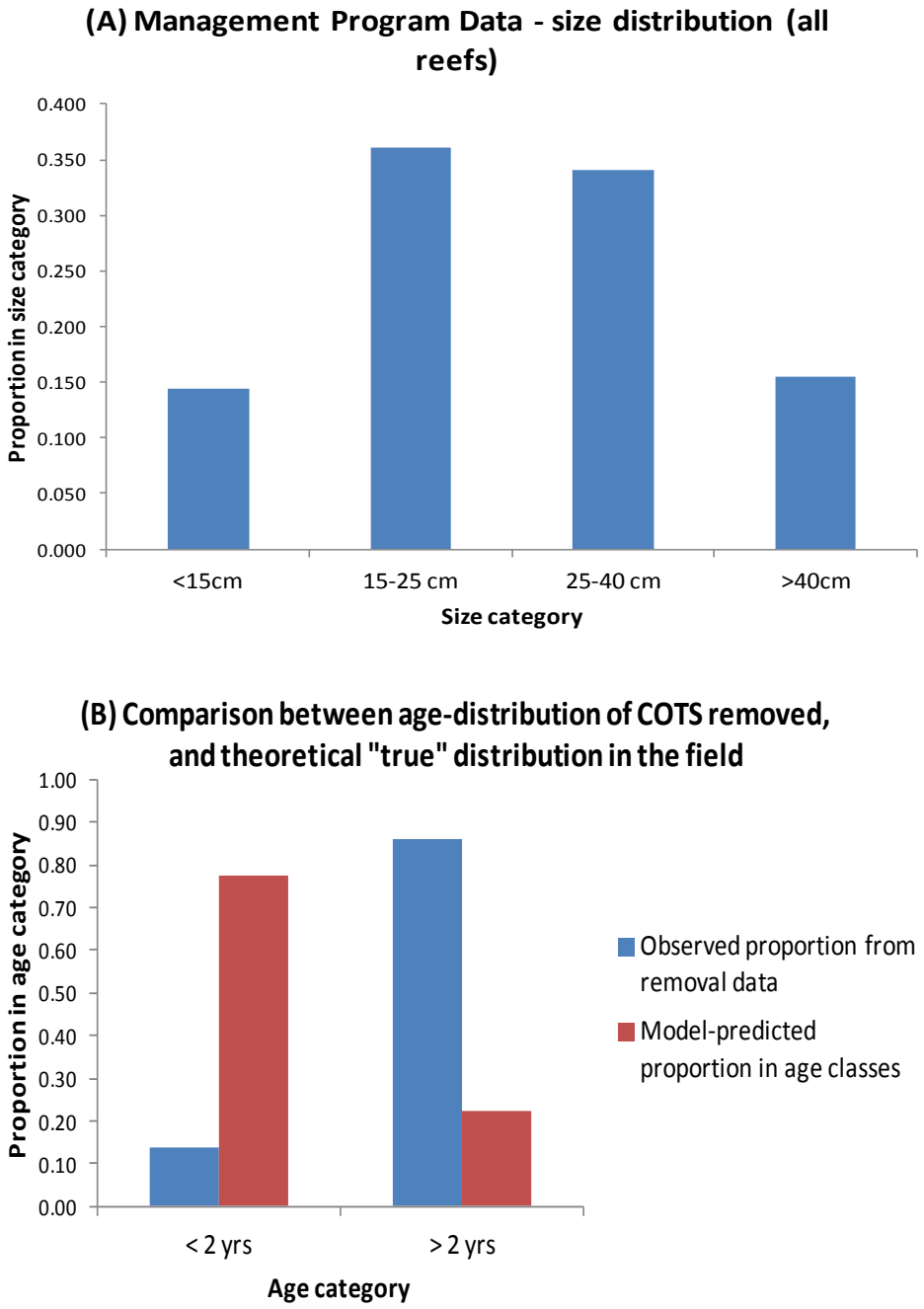

Figure 3.2 (A) Summary of COTS management program size distribution of COTS from all reefs, and (B) preliminary conversion to relative age proportions for comparison with model-derived age distribution.

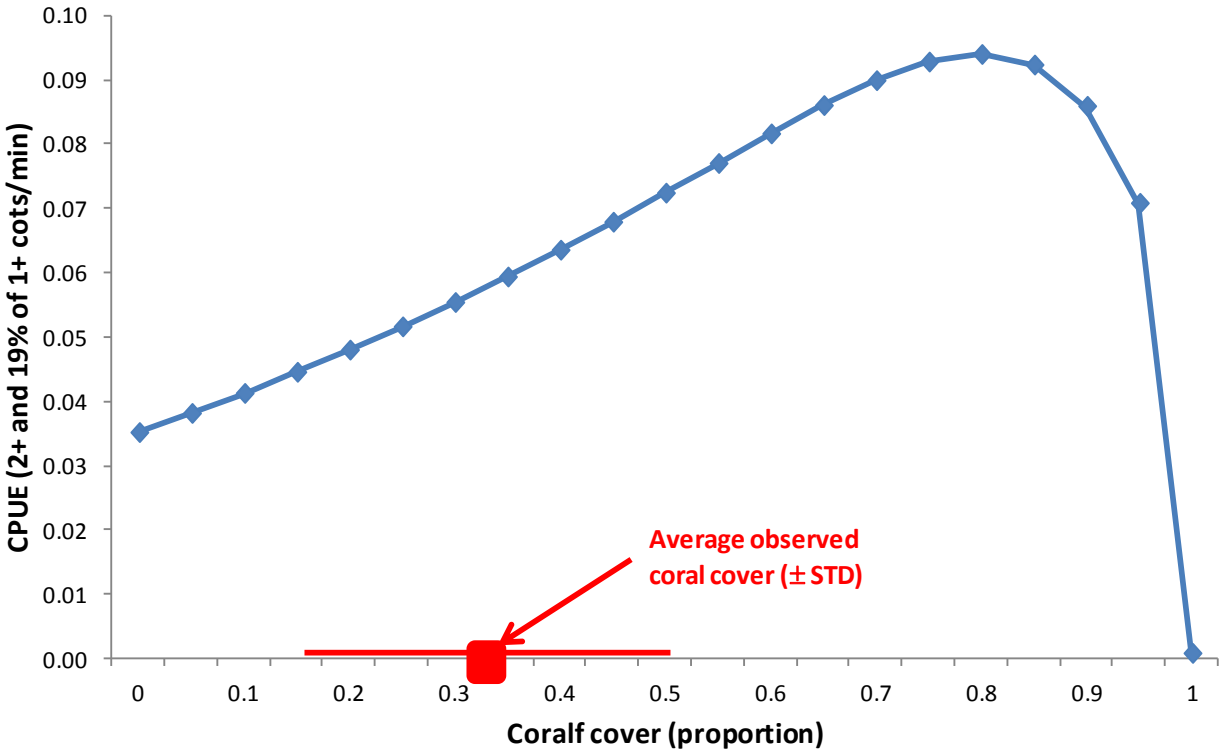

Figure 3.3 Model-derived relationship between CPUE and fast-growing coral (Coralf) proportion. The average observed coral cover (+ STD) recorded in the management program database is shown for comparison on the horizontal axis. The vertical axis units are those which correspond most closely to the units of the CPUE measures recorded in the field, namely the total of all age 2+ COTS individuals plus 19% (the selectivity) of the age 1+ COTS removed per minute (see text).

4 Question 2B: Enabling net growth in coral cover: what is the COTS outbreak threshold?

4.1 Summary and Key Conclusions

- A spatially expanded version of the Morello et al. (in press) COTS model was used to further explore the findings (reported in an earlier progress report) that at higher coral cover levels, more COTS are needed to reduce the coral cover below equilibrium and thus to investigate the effect of initial coral levels on the effectiveness of manual removal/poison injections.
- Initial coral levels are expressed in relative terms as the percentage of coral (fast- and slow-growing) carrying capacity.
- The spatially expanded model (two reefs) was developed within the framework of a separate project. It was used as the starting point for carrying out twenty-year deterministic projections into the future, simulating the effect of manual lethal injection of different proportions of age 1 and age 2+ COTS (in the absence of predation) at different levels of coral.
- The results show that both increasing the selectivity of COTS age 1+ and/or the proportion of total COTS removed, proportionally decreases the effects COTS have on coral. The proportion of the younger age 1+ animals that are removed is very influential in determining the success of removals. But it is the initial coral level that appears to be the most important factor, and hence the model simulations suggest that it is important to account for this when assessing removal rates that are required to stall or reverse declines in coral cover due to damage from COTS.
- Both the proportion of COTS removed and initial coral cover have a substantial effect on the average number of years taken for fast-growing coral to recover (Figure 4.5). For example it is estimated that if the initial coral level were 20% of its carrying capacity, then it would take an average of 11.5 years for fast-growing coral to recover even when 50% of all COTS aged 1+ are removed and the selectivity of age 1+ COTS is 100%. This compares to a much shorter average recovery period of 7.5 years under a 50% initial coral cover scenario combined with the assumption that 50% of COTS aged 1+ are removed (assuming the selectivity of age 1+ COTS is 50%) (Figure 4.5, Table 4.5). This is largely because net coral growth rate is slow when coral cover is low. Recovery times would also vary depending on the density of the outbreak.

4.2 Introduction

The growth of both fast-growing and slow-growing coral is negatively affected by COTS consumption. The results of a steady state analysis based on the model described in Morello et al. (in press) suggest that if coral cover is high, then the same number of COTS will have less impact on the system than would be the case at lower levels of coral cover (Section 3). This means that more COTS are needed to reduce the coral cover below equilibrium at higher coral cover levels: for example, if the coral cover is 80%, then the model suggests that as many as 20 COTS ha^{-1} (2+ animals) can be sustained without causing a further decline in the (fast-growing) coral cover, compared with 9 COTS ha^{-1} when the coral cover is 40%, and 5 COTS ha^{-1} when the coral cover is 20%. The aim of the work summarised in this chapter was to use a spatially expanded version of the COTS model to further explore these findings in a dynamic rather than equilibrium context, and to investigate the effect of initial coral levels on the effectiveness of manual removal/poison injections.

4.3 Methods

4.3.1 EXPANDED COTS MODEL

This version of the model is expanded with respect to the one described in Morello et al. (in press). This work was carried out as part of a separate project which foresaw the addition of a spatial dimension to the original model by progressively increasing the number of reefs modelled, starting from one extra reef. To

do this, we allowed the two reefs, Lizard Island and Horseshoe reef, to share all parameters with the exception of COTS self-recruitment and immigration which were specified and estimated separately (Table 4.1). Similarly to Lizard Island, the data for Horseshoe reef were collected within the framework of the AIMS Long Term Monitoring Program (LTMP; Sweatman et al. 2008). The main results of this new model fit are illustrated in Figure 4.1, and the estimated parameters are summarised in Table 4.2.

4.3.2 SIMULATIONS OF COTS REMOVALS

This two-reef model was used as the starting point for the work described herein. Thus, for the purpose of answering our question, based on the two-reef model described above, we carried out twenty-year deterministic projections into the future starting in 2011. We simulated and evaluated the effect of manual lethal injection of different proportions of age 1 and age 2+ COTS (in the absence of predation) at different levels of initial coral (10%, 20% and 50%). These initial levels of coral (fast- and slow-growing) are expressed in relative terms as a proportion of coral (fast- and slow-growing) carrying capacity. Coral carrying capacity is assumed to be 100% cover. Simulations were run across a broad range of hypothetical manual removal intensities. For simplicity we projected a single outbreak peak into the future, the immigration peak.

4.4 Results and Discussion

The results are similar for the two reefs, Lizard and Horseshoe, and examples are shown for a single reef only, Horseshoe reef. Note that in both cases the model estimates the parameter set that best explains a historic COTS outbreak, and hence the model can be forward projected to either replicate the outbreak pattern, or to investigate what the effect is on COTS abundance and coral cover of alternative management scenarios.

Figure 4.2 summarises the results obtained for Horseshoe Reef when investigating the combined effects of different values of:

- “Fsel”: the selectivity of age 1 COTS, i.e. the proportion of age 1 COTS available for removal, and
- “Fremove”: the proportion of both the age 1 COTS available and the age 2+ COTS. It is assumed that all age 2+ COTS are available for removal: their selectivity is 1.

The different combinations investigated are summarised in Table 4.3.

This first set of simulations shows that progressively increasing the proportion of COTS age 1 available for removal and the proportion of 2+ COTS removed, proportionally decreases the effects COTS have on coral. But it is the availability of COTS of age 1 to capture that really determines the success of removals. The time taken for both types of coral to recover is illustrated for Horseshoe reef in Figure 4.3, showing that recovery of fast-growing coral was fastest when more COTS were removed, and recovery of massive corals took very much longer.

Figure 4.4 summarises the results obtained when investigating the effects of different values of initial coral levels on the effectiveness of manual removals for selected combinations of Fsel and Fremove (Table 4.4)

This second set of simulations shows that the more depleted (with respect to carrying capacity) the initial coral population is, the more severe the effect of COTS on the population trajectory of both coral types. Initial coral levels appear to be a more important determinant than the proportion of COTS removed.

The combination of the proportion of COTS removed and the coral levels at the start of the outbreak both influence the average number of years taken for fast-growing coral to recover (Figure 4.5). It is estimated that if the initial coral were 20% of carrying capacity, then it would take an average of 11.5 years for fast-growing coral to recover when 50% of all COTS aged 1+ (i.e. COTS of age 1 and age 2+) are removed and the selectivity of age 1 COTS is 100%. This is compares to an average of 7.5 years if the initial coral were 50% of carrying capacity and 50% of COTS aged 1+ are removed and the selectivity of age 1 COTS is 50% (Figure 4.5, Table 4.5). Recovery times would also vary depending on the density of the outbreak.

Table 4.1 Input parameters for the two-reef COTS model

Parameter	Description	Value	Rationale / Notes
COTS			
$COTS_{init}$	Initial number of 2+ COTS	Estimated	The numbers of age 1+ and age 0 COTS are computed by multiplying the value of $COTS_{init}$ by $e^{M^{Cots}}$ and $e^{2M^{Cots}}$ respectively.
ε_y^L	Lizard Island stock-recruitment residual for year *y*	0 for all years except 1996	The value for 1996 is estimated
ε_y^H	Horseshoe reef stock-recruitment residual for year *y*	0 for all years except 2001	The value for 2001 is estimated
I	Median background immigration	1	
η_y^L	Lizard Island immigration residual for year *y*	0 for all years except 1994	The value for 1994 is estimated
η_y^H	Horseshoe reef immigration residual for year *y*	0 for all years except 1996	The value for 1996 is estimated
h	Stock-recruitment steepness	1	Implies that self-recruitment is constant in expectation
R_0	Unfished recruitment	1	
K^{Cots}	Carrying capacity	N/A	Does not impact the dynamics given the assumed value for *h*
M^{Cots}	Natural mortality	Estimated	
p_1^{Cots}	Predation effect of large fish on COTS	0	Non-zero values are considered in the projections
p_2^{Cots}	Predation effect of large fish on COTS	50	Pre-specified as it is correlated with p_1^{Cots}
$\tilde{p}$	Effect of fast coral on COTS mortality	Estimated	
N_c	Saturation parameter	0.5	Pre-specified after initial model tuning
μ	Saturation parameter	5	Set so that there is a rapid switch between fast-growing and slow-growing coral when coral biomass drops below N_c
ω	Mortality estimated by fitting the model	2.560yr^{-1}	Natural mortality estimated by the base case model
λ	Parameter controlling the difference between mortality rates of younger and older animals	0.1, 0.2, 0.3, estimated	Parameter λ can be either estimated or fixed to a constant
Fast-growing coral			
C_{init}^f	Initial biomass	Set to K^f	
r^f	Intrinsic rate of growth	0.5 yr^{-1}	Pre-specified after initial model tuning
K^f	Carrying capacity	2500	Arbitrary*
p_1^f	Effect of COTS on fast-growing coral	Estimated	
p_2^f	Effect of COTS on fast-growing coral	10	Pre-specified as it is correlated with p_1^f
Slow-growing coral			
C_{init}^m	Initial biomass	Set to K^m	
r^m	Intrinsic rate of growth	0.1 yr^{-1}	5-fold lower than for fast-growing coral
K^m	Carrying capacity	500	Arbitrary*

p_1^m	Effect of COTS on slow-growing coral	Estimated	
p_2^m	Effect of COTS on slow-growing coral	8	Pre-specified as it is correlated with p_1^m

Table 4.2 Two-reef model base-case parameter estimates and Hessian-based standard errors

Parameter	Description	Value	SD	CV
COTS				
$COTS_{init}$	Initial number of 2+ COTS	0.300	0.013	0.044
ε_y^L	Lizard island stock-recruitment residual for year 1996	3.866	0.080	0.020
η_y^L	Lizard Island immigration for year 1994	4.053	0.118	0.030
ε_y^H	Horseshoe reef stock-recruitment residual for year 2001	4.171	0.069	0.017
η_y^H	Horseshoe reef immigration for year 1996	3.720	0.125	0.034
M^{Cots}	Natural mortality rate	2.772	0.020	0.007
Fast-growing coral				
p_1^f	Effect of COTS on fast-growth coral	0.067	0.003	0.048
$\tilde{p}$	Effect of fast-growing coral on COTS	0.595	0.022	0.037
Slow-growing coral				
p_1^m	Effect of COTS on slow-growth coral	0.085	0.007	0.087

Table 4.3 Simulation runs undertaken to investigate the effects of making different proportions of age 1 COTS available for removal (Fsel) and removing different proportions of age 1 and age 2+ COTS (Fremove)

Fsel	Fremove	Fremove*Fsel
1	0.2	0.2
1	0.5	0.5
1	0.9	0.9
0.5	0.2	0.1
0.5	0.5	0.25
0.5	0.9	0.45

Table 4.4 Simulation runs undertaken to investigate the effects of making different proportions of age 1 COTS available for removal (Fsel) and removing different proportions of age 1+ and age 2+ COTS (Fremove) at different levels of initial coral, expressed as a percentage of carrying capacity

Fsel	Fremove	Fremove*Fsel	Initial level of coral (% of carrying capacity)
1	0.5	0.5	10
1	0.5	0.5	20
1	0.5	0.5	50
0.5	0.5	0.25	10
0.5	0.5	0.25	20
0.5	0.5	0.25	50

Table 4.5 The estimated time taken (years) for fast-growing (Coralf) and massive (Coralm) coral to recover from COTS outbreaks at different levels of removal (Fremove*Fsel = 0.25, 0.5) and different levels of initial coral (proportion of coral carrying capacity = 0.1, 0.2, 0.5) at Lizard Island and Horseshoe reef.

					Lizard island		Horseshoe reef	
Fremove	**Fsel**	**Fremove*Fsel**	**Initial level of coral**	**ID**	**Coralf**	**Coralm**	**Coralf**	**Coralm**
0.5	1	0.5	0.1	0.25_0.1	14	20	11	20
0.5	1	0.5	0.1	0.5_0.1	13	20	11	20
0.5	1	0.5	0.2	0.25_0.2	13	20	10	20
0.5	1	0.5	0.2	0.5_0.2	11	20	9	20
0.5	0.5	0.25	0.5	0.25_0.5	11	20	8	9
0.5	0.5	0.25	0.5	0.5_0.5	9	20	6	8

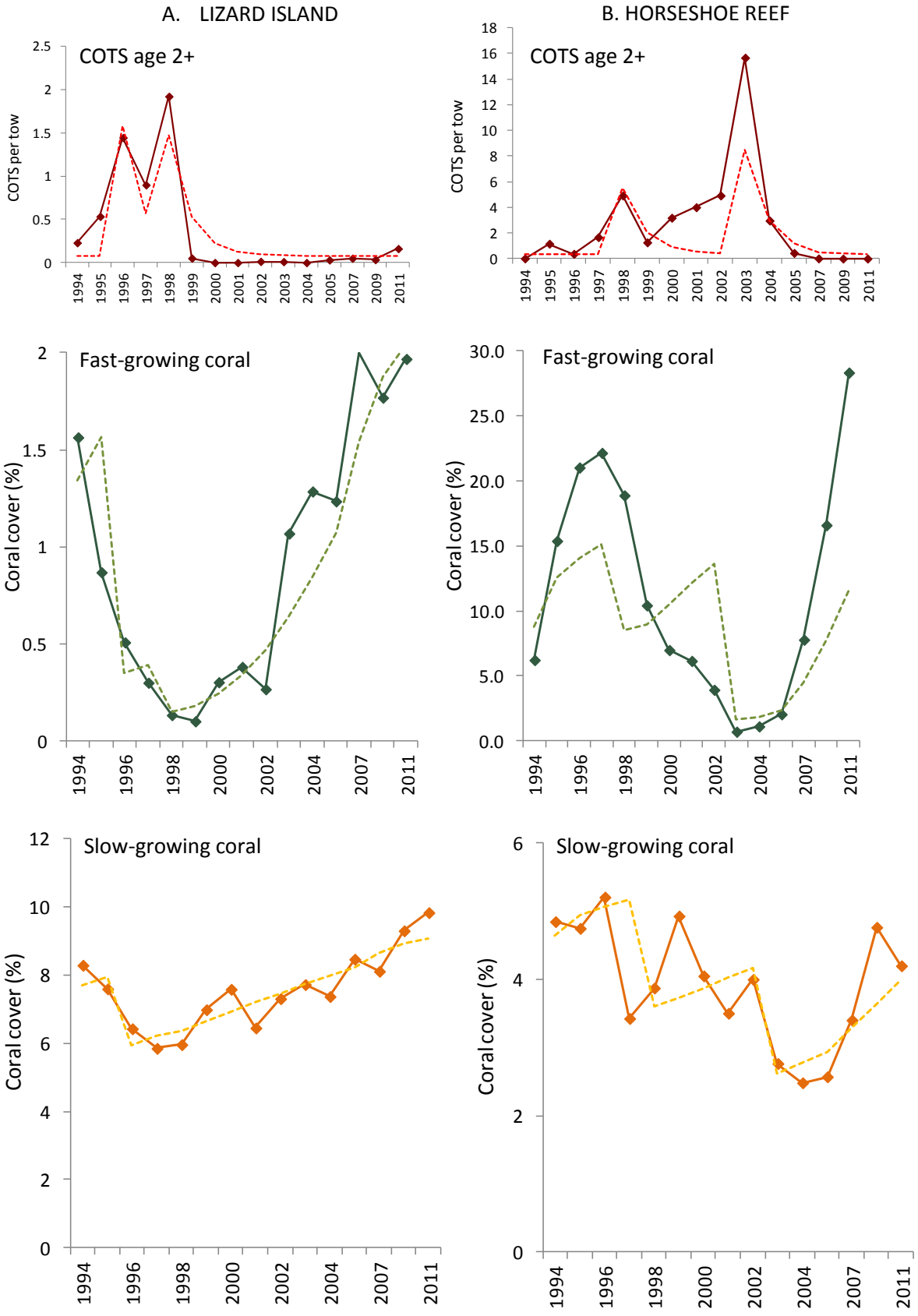

Figure 4.1 Observed data (symbols and solid line) for COTS adults (red), fast growing coral (green) and slow-growing coral (yellow) from (A) Lizard Island and (B) Horseshoe Reef from 1994 to 2011 and the respective values estimated by the model when fitted to these data (dashed lines)

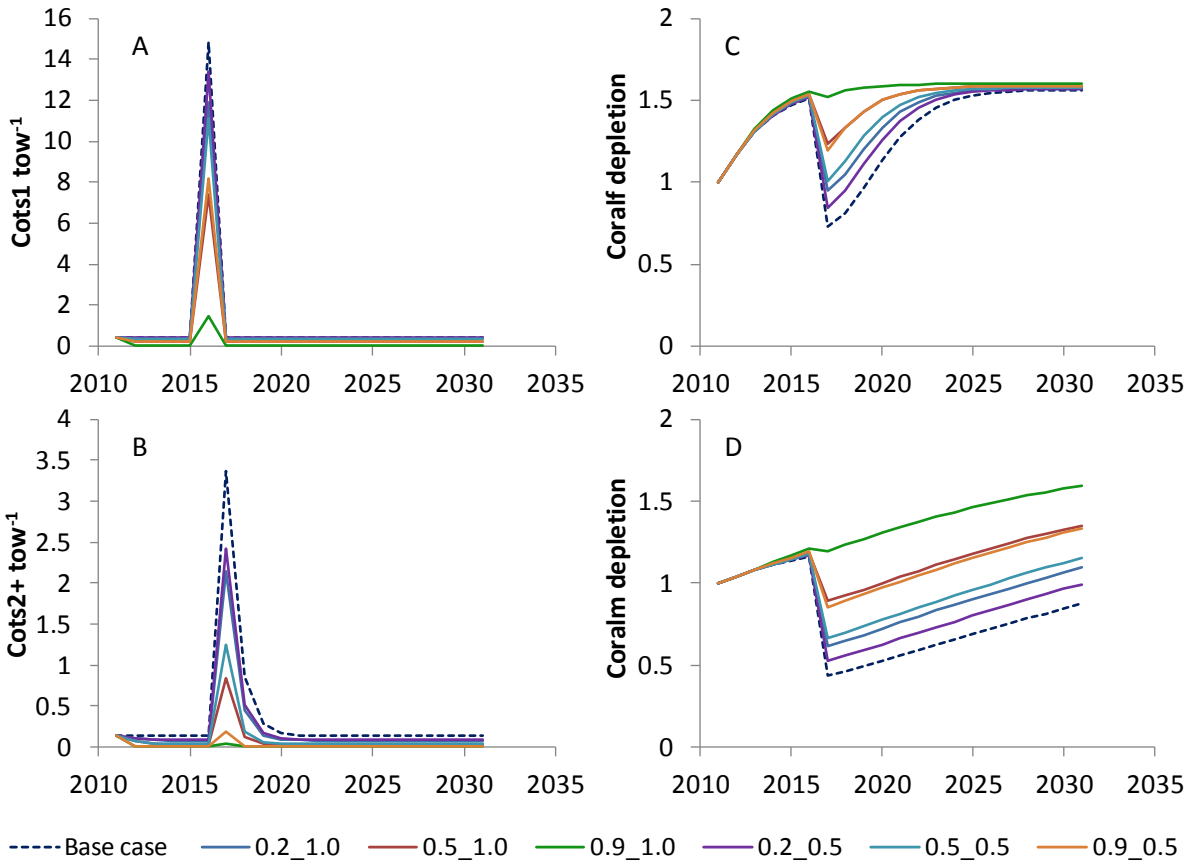

Figure 4.2 Results of the projections (2011 – 2031) for Horseshoe Reef (simulating the immigration peak only) showing the effect of availability on manual removal of different proportions of age 1 COTS (Fsel) and age-1+ COTS (Fremove) on (A) age 1 COTS, (B) age-2+ COTS, and depletion (*cfr* initial coral cover) of (C) fast-growing coral and (D) slow-growing coral. For combinations of parameters simulated refer to Table 4.3

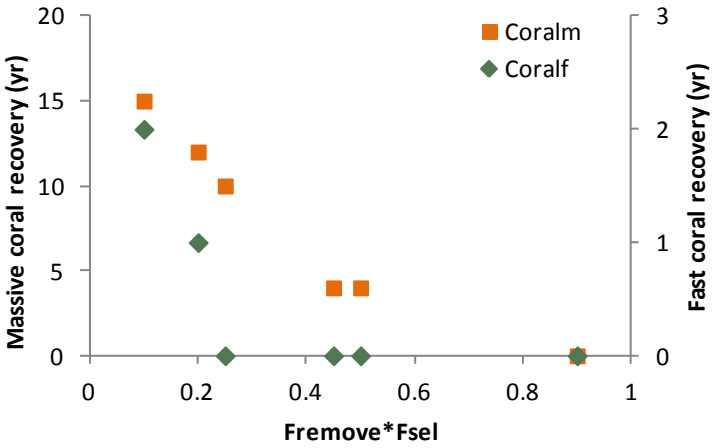

Figure 4.3 The time taken for massive (Coralm) and fast-growing (Coralf) coral to recover from COTS outbreaks at different levels of removal at Horseshoe reef. For combinations of parameters simulated refer to Table 4.3.

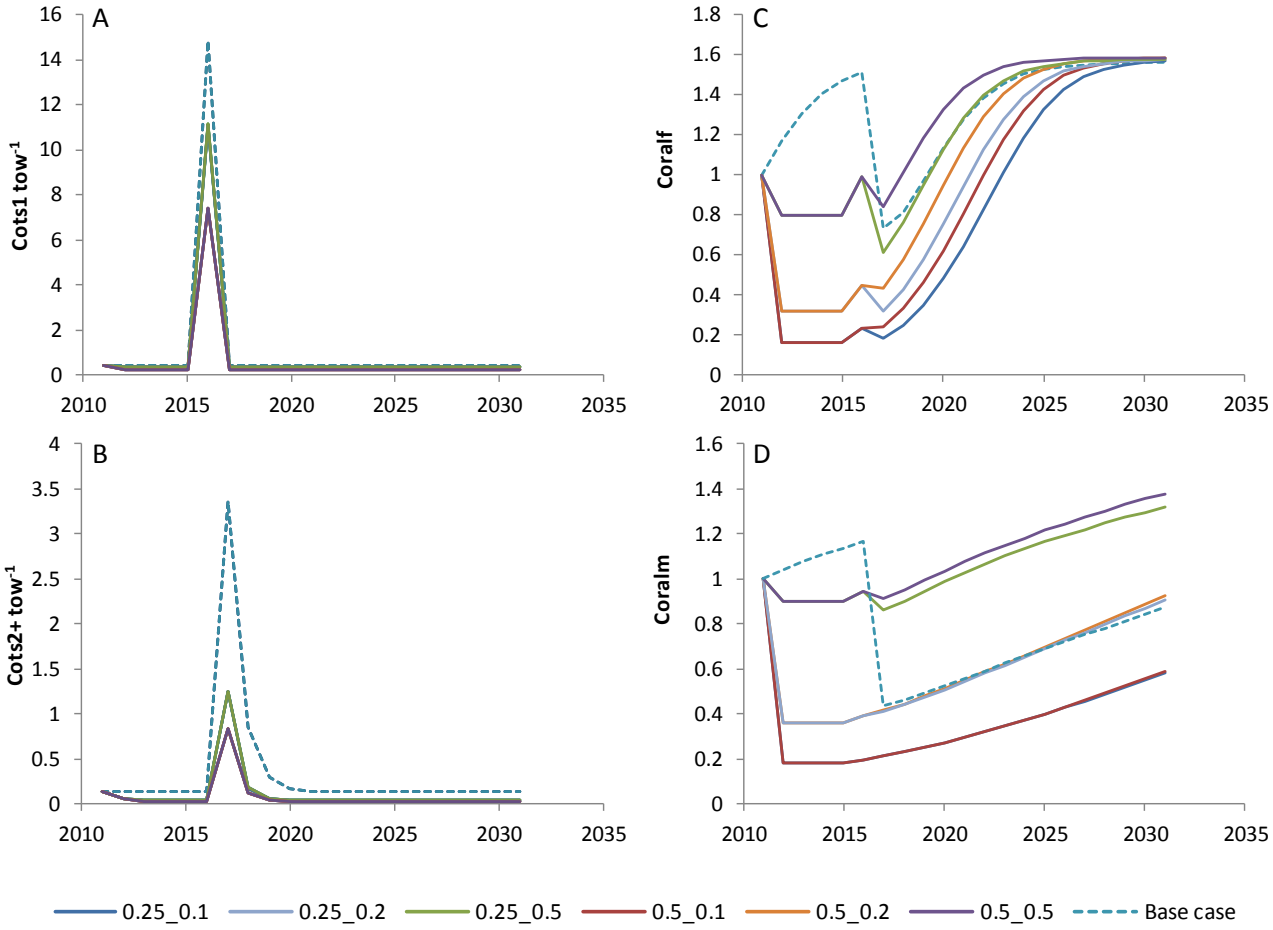

Figure 4.4 Results of the projections (2011 – 2031) for Horseshoe Reef (simulating the immigration peak only) showing the effect of different combinations of availability*manual removal of different proportions of age 1 COTS (Fsel), and age-2+ COTS (Fremove) and of initial levels of coral (10%, 20%, 50% of coral carrying capacity) on (A) age 1 COTS, (B) age-2+ COTS, and depletion (proportion of initial coral cover – *K*) of (C) fast-growing coral and (D) slow-growing coral. For combinations of parameters simulated refer to Table 4.4.

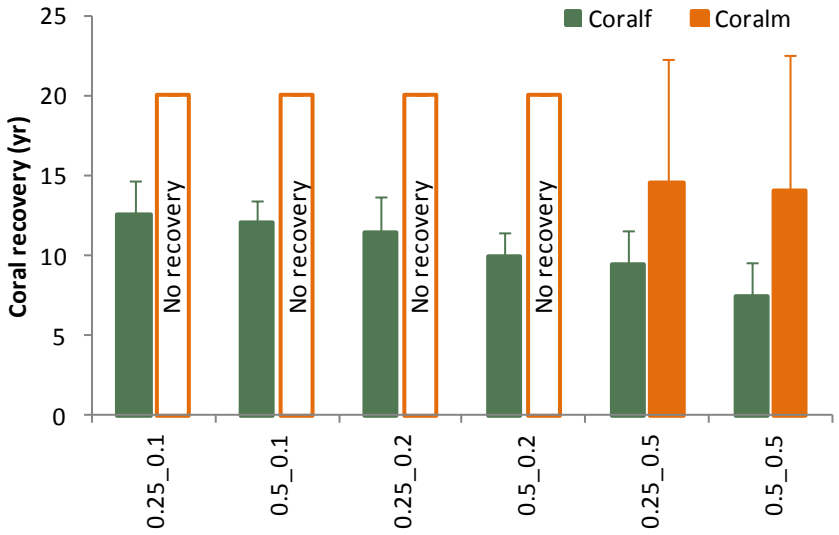

Figure 4.5 The mean time taken (years + standard deviation) for massive (Coralm) and fast-growing (Coralf) coral to recover from COTS outbreaks at different levels of removal (Fremove*Fsel = 0.25, 0.5) and different levels of initial coral (10%, 20%, 50% of coral carrying capacity). For combinations of parameters simulated refer to Table 4.5 ("ID"). "No recovery" refers to a longer timeframe for full recovery needed than the 20-year projection period.

5 Question 3: What is the relationship between COTS density and the reproductive potential of the population in terms of (i) fertilization success rate and (ii) overall larval production?

5.1 Introduction

Numerous hypotheses have been put forward to explain the occurrence of population outbreaks of *Acanthaster* spp. (reviewed by Moran 1986, Birkeland & Lucas 1990, Pratchett et al. 2014), including the 'natural causes hypothesis' (Vine 1973), and 'adult aggregation hypothesis' (Dana et al. 1972) both of which emphasize the faustian traits of *Acanthaster* (e.g. phenomenal reproductive capacity, rapid growth; Birkeland 1989) that predispose them to major population fluctuations. The essence of these hypotheses is that if COTS aggregate for any reason, for example around residual food sources after events such as cyclones, or at high population densities, their reproductive success may increase greatly. This is because COTS are free-spawners and sperm dilution and gamete dispersal may be a factor limiting reproductive success for free spawning invertebrates under most conditions (e.g. Levitan 1991). This is one process through which Allee effects (density dependent limitation in reproductive success) may manifest in such species.

Theories of COTS outbreaks such as the Natural Causes hypothesis, in combination with a renewal of interest in theoretical and empirical aspects of fertilization ecology in the mid-late 1980s (e.g. Pennington 1985), led the Crown-of-thorns Starfish Research Committee (COTSREC) to support research to investigate key features influencing Allee effects on COTS. This work included both laboratory (Benzie et al. 1994, Babcock and Mundy 1993) and field based studies (Babcock et al. 1993, Mundy et al. 1994, Benzie and Dixon 1994) of gamete properties, gamete interactions, in situ fertilization rates and natural spawning behaviour. These studies greatly advanced our knowledge of COTS reproductive biology and ecology, providing systematic observations of natural spawning as well as quantitative estimates of many critical gamete properties. Perhaps most surprising was the capacity of COTS to achieve successful fertilization at distances orders of magnitude greater than those measured in other invertebrates (Babcock et al 1993). For example fertilization was over 20% with a 60m separation of males and females, and still 6% for females 100m downstream from a spawning male. In contrast similar experiments with sea urchins showed that fertilization dropped to essentially zero after only 1m (Pennington 1985). This observation appeared to lend credence to the possibility that reproduction was in some way implicated in COTS propensity for population outbreaks.

By the time COTSREC funding had come to an end, this work on COTS reproductive ecology had left us tantalizingly close to being able to extend these results to the population level. However while it was possible to estimate levels of reproductive success in the laboratory or in controlled experimental conditions on the reef, it was not possible to extrapolate these results in a quantitative manner to COTS populations. To do this a spatially explicit COTS population model was required, including sperm and egg diffusion and gamete interactions. With such a model the density and distribution of COTS, plus the timing and synchrony of spawning could all be accounted for to produce estimates of not only fertilization success but also for zygote/larval production in populations of a given density. Only then would it be possible to provide quantitative estimates of density thresholds for reproductive success that could be compared with actual starfish densities on a range of reefs, allowing more rigorous evaluation of theories such as the "Natural Causes" hypothesis. Answers to these questions are also of crucial importance in long-term

attempts to control COTS populations, and maintain them at densities below which they will not spawn ongoing series of outbreaks.

Here we have assembled the data from the literature in order to construct a mathematical model of fertilization success in COTS populations that would allow us to begin to produce quantitative answers to the following questions crucial to understanding and managing COTS outbreaks:

> What is the relationship between COTS density and the reproductive potential of the population in terms of (i) fertilization success rate and (ii) overall larval production?

5.2 Methods

5.2.1 DIFFUSION MODEL

We used a stochastic individual-based simulation model of COTS to quantify the relationship between COTS density and the reproductive potential of the population in terms of (i) fertilization success rate and (ii) overall larval production. Our model is based on empirical fertilization data from Babcock et al. (1994) and other sources as summarised in Table 5.1 (Diffusion model), Table 5.2 (Fertilization model) and Table 5.3 (Spawning ecology).

Empirical measures of fertilization rate were obtained in experimental spawnings of reproductively mature starfish that were induced by injections of 1-methyl adenine. Male starfish were located upstream of spawning female starfish, which were placed at varying distances downstream of the males (Babcock et al. 1994). Eggs were sampled using a submersible plankton pump, with discrete samples contained in individual cartridges (Mundy and Babcock 1994). This pump was also used to sample gametes during natural spawnings. Fertilization rates scored from these samples were used to tune a sperm-diffusion fertilization model of reproductive success (Babcock et al. 1994). This model realistically predicted fertilization rates for pairs of spawning starfish when males were situated at known distances upstream from females.

Here we have modelled the shedding of sperm into a flow as a plume diffusion problem, based on the approach of Babcock et al. (1994). This assumes the water column is moving at a mean velocity *U* parallel to the *x*-axis within a turbulent benthic boundary layer. Each individual male or female COTS is assumed to be a point source at the *x,y* origin and at an equal distance *h* above the substratum, shedding sperm and eggs respectively at constant rates *Qs* and *Qe.* The resulting sperm concentration *S* (or equivalently egg concentration *E*) at points (*x,y,z*) away from the source emission is given by:

$$S(x,y,z) = \left(\frac{Qs}{2\pi U \sigma_y \sigma_z}\right)\left\{\exp\left(-y^2/2\sigma_y^2 - \left(\frac{(z-h)^2}{2\sigma_z^2}\right)\right) + \exp\left(-y^2/2\sigma_y^2 - \left(\frac{(z+h)^2}{2\sigma_z^2}\right)\right) + \exp\left(-y^2/2\sigma_y^2 - \left(\frac{2(d-z-h)^2}{2\sigma_z^2}\right)\right)\right\}$$

Eqn 5.1

where parameter definitions and values are shown in Table 5.1. Eqn 5.1 incorporates an adjustment to account for the reflection of sperm from the surface back into the flow in water of depth *d*. Sensitivity to alternative parameter settings is also investigated. We assumed an equal sex ratio (Table 5.3), synchronous spawning and that COTS are randomly spaced. Moreover, we assume that most spawning COTS will be at a similar depth (or equivalently distance from the substratum) on a reef, but if there is a significant vertical difference in their distribution, then our calculations will slightly overestimate fertilisation success.

The model focus area was a grid measuring 100m x 100 m (1 hectare), divided into 2mx2m cells (Figure 5.1). Given that field measurements indicated a large scale (100m) at which the effects of sperm diffusion were observed for *Acanthaster*, we expanded the model grid to account for boundary conditions, such as accounting for sperm from neighbouring individuals beyond the boundaries of the focus area. Hence the total model area was 200m x 200m (divided into 100 x 100 = 10 000 cells) but because of the assumption of

a downstream flow transporting eggs and sperm, the boundary areas were explicitly simulated upstream and to the sides of the model focus area, but not downstream from the model focus area. Hence a boundary rectangle measuring 100m in the upstream direction and 200m cross-stream was situated upstream of the focus area, and a boundary rectangle measuring 100m in the downstream direction and 50m in the cross-stream direction was situated to either side of the focus area to account for eddies that disperse the plume as it spreads out (Figure 5.1).

5.2.2 FERTILISATION SUCCESS RATE MODEL

The number *n* of COTS in the model area was successively increased from 2 animals to 800 animals (with equal numbers of males and females), and the density of spawning individuals computed in units of spawning individuals per hectare, assuming a maximum proportion spawning as per Table 5.3. The total number of sperm and eggs in each of the model cells after time *t* was then used to compute the percent fertilisation success *F* at each point using the relation:

$$F(x,y,z) = 1 - \exp\left(-\theta S t u^{*}\right) \qquad \text{Eqn 5.2}$$

with parameter values as shown in Table 5.2. The reference time period *t* used was 2700 s, which accounts for the duration of spawning as well as the duration of gamete viability and transport time under prevailing current conditions (Babcock et al. 1994, Benzie and Dixon 1994).

For each COTS density in the range 2-800, we ran 500 simulations with random placement of spawners. The number of simulations was chosen based on examination of convergence of model results as a function of the number of simulations, but we also ran an example with 2000 simulations to cross-check our results. For each simulation at a pre-specified COTS density, we computed the average fertilisation success in the model focus area (i.e. averaged across 2500 cells). Next we computed both the average and standard deviation of the fertilisation success percentages from all simulations and plotted this as a function of the COTS density.

5.2.3 QUANTIFYING ZYGOTE PRODUCTION

To calculate the relative number of zygotes *Z* produced in each simulation for each density of COTS, we used the following equation:

$$Z(x,y,z) = \sum_{x=1}^{50}\sum_{y=1}^{50} F(x,y,z) \times \mathrm{E(x,y,z)} \qquad \text{Eqn 5.3}$$

We therefore computed the sum of the number of fertilised eggs in the model focus area, taking into account both the fertilisation success probability as well as the number of eggs actually spawned at each location. We compute the average and standard deviation of the total zygotes from all simulations. We then use the zygote numbers as a relative index of population level reproductive success and larval production plotted as a function of COTS density.

5.2.4 SENSITIVITY ANALYSES

The sensitivity of the model was tested to a range of alternative values for the following parameters:
$u^{*}, \overline{U}, t, Q_e$

U*=0.05 (base); 0.10;

U=0.12 (base); 0.06; 0.18

T=2700s, t=30; t=1800

Qe = 10^7 (base); 10^4

5.2.5 SHAPE OF THE ZYGOTE PRODUCTION CURVE AND TESTING FOR AN ALLEE EFFECT

We analysed the shape of (1) the fertilisation rate (%), and (2) the zygote production curve (y) as a function of COTS density (x) (focusing on low population density scenarios) to test whether there is any evidence for an Allee effect whereby zygote production drops precipitously below a threshold level of density. The alternative hypothesis tested is that zygote production decreases linearly to zero as population density decreases to zero. We fitted three alternative functional forms to each of the model results for fertilization rate and zygote production above, as follows:

$$(a)\, y = ax + b$$

$$(b)\, y = ax^b$$

$$(c)\, y = a \cdot \exp(bx)$$

Hence we tested whether the relationships above are best described by a (a) simple linear relationship; (b)(i) power curve with a convex upward shape (parameter $b > 1$) or (ii) asymptotic shape ($b<1$) or (c) exponential function. Both a power curve with power $b>1$ and an exponential curve with $b>0$ have a convex upward shape which is suggestive of an Allee effect because fertilization and/or zygote production drops more steeply than linearly as the curve approaches the origin (Figure 5.2). Although we could have fitted more complex curves (such as a logistic or negative exponential, both of which require estimation of 3 rather than 2 parameters), our preference was start with the simplest possible model with the advantage that each of our options requires estimation of two parameters only. Moreover, the purpose of determining the shape of the curve was not to obtain a representation of the entire zygote production curve, but only the shape at low population density to test whether or not the curve is linear. Note also that more complex formulations such as a logistic sigmoid-shape curve have an exponential shape as one approaches the origin. We ran our analyses using first 58 values (COTS densities from 0.34 up to 20 COTS ha^{-1}). We also reran the analysis to test using the first 80 values (COTS densities from 0.34 up to 27 COTS ha^{-1}), and the results were the same and hence these are not also shown. We coded all our models in AD Model Builder and computed Hessian-based standard error estimates (Fournier et al. 2012).

5.3 RESULTS

Figure 5.3 shows examples of single model simulations of sperm plumes over an area of one hectare with different numbers of initial COTS up to a maximum of 20. Figure 5.4 illustrates the corresponding zygote plumes.

The base-case model results for the fertilisation success rate as a function of COTS spawning density (number per hectare) is shown in Figure 5.5. The curve resembles a Beverton-Holt stock-recruitment type curve with fertilization rates changing most rapidly at densities around 10 COTS ha^{-1} and 50% fertilization rate achieved at between 8 and 9 COTS ha^{-1}. In contrast the model-predicted zygote production (+ std) as a function of COTS density has a different shape (Figure 5.6). In both instances 5000 simulations were run at each of a range of COTS densities from low densities up to high densities of 80 COTS ha^{-1}. The average values and coefficient of variation (CV) computed across all the simulations were similar when fewer simulations were run, and hence all other results presented are based on 1000 simulations (to save run time). Although these runs were conducted using densities up to 34 spawning COTS ha^{-1}, the focus of this analysis was on the patterns at lower COTS density and hence, to aid visualisation, plots are shown for COTS densities up to 20 COTS ha^{-1} (Figure 5.7 and Figure 5.8). We use zygote production as our index of population level reproductive output, and will analyse these curves for evidence of an Allee effect. In Figure 5.8, reproductive outputs seem to drop off around 17-18 COTS ha^{-1} and drop to still lower levels around 13 COTS ha^{-1}.

For the base-case value of the shear velocity parameter u* that we used (0.05), there appears to be an exponential increase in zygote production with increasing cots density (Figure 5.8) i.e. Allee-type effect (this is more formally tested in the next section). The model was sensitive to the choice of the parameter u* and hence results were also tested using alternative values. If u* is large (e.g. 0.1), suggesting greater shear velocity/turbulence assumptions, then the relationship appeared approximately linear with increasing COTS density (Figure 5.9).

5.3.1 SENSITIVITY ANALYSIS

The base-case model used a time period of 2700 seconds over which to compute fertilisation success and zygote production. This value was based on a number of considerations, including the emission time from the point source and gamete viability time, and hence the model results reflect the final maximum outcomes. The increase in zygote production with increasing time t is shown in Figure 5.10. The effect of changing the egg release rate parameter Q_e was simply to linearly scale the zygote production in sync, because in Eqn 3.3 the zygote production is linearly related to values of Q_e. Thus the egg release rate doesn't change the shape of the overall relationship but is an important parameter if the magnitude of zygote production needs to be known.

The model was relatively insensitive to alternative values of the mean current velocity parameter (Figure 5.11), but highly sensitive to alternative choices for u*, as discussed above (Figure 5.9).

5.3.2 SHAPE OF THE ZYGOTE PRODUCTION CURVE AND TESTING FOR AN ALLEE EFFECT

The parameter estimates when fitting alternative functions to the shape modelled data near the origin are shown in Table 5.4, and Figure 5.12 shows the fitted curves for fertilization success and Figure 5.13 for zygote production plotted as a function of COTS density. Statistically the preferred model in the case of fertilisation success is a power curve, but the shape parameter b is < 1 (termed asymptotic for current purposes). In the case of zygote production, the preferred model is an exponential model, suggesting an exponential relationship best describes the relationship of zygote production and COTS density (Figure 5.13).

As illustrated in Figure 5.12, the relationship between fertilization success and COTS density is thus roughly linear when close to the origin, but the power shape means that fertilization decreases far more at low densities than at high densities. In contrast, the best-fit shape parameter b for zygote production is substantially larger than one, suggesting a concave shape and in this case the exponential function is the preferred model. Clearly therefore in the case of zygote production there is no evidence that recruitment decreases linearly to zero as population density decreases to zero. Hence interpreting these results conservatively, we reject the hypothesis of an Allee-type relationship between fertilisation success percent and COTS abundance at low stock density, but we accept the hypothesis of an Allee-type relationship between zygote production and COTS abundance at low stock density. Based on our model, it therefore seems plausible that COTS may show an Allee-type relationship in their overall zygote production when considering the concentrations, dispersion and overlaps of sperm and ova that are shed into the water from these broadcast spawners.

However our results also suggest that this result does not hold under all circumstances. For example, under the Sensitivity scenario that uses a larger value for u* (namely 0.10), the shape of the zygote production versus COTS density relationship was best described by a linear relationship (Table 5.4(C), Figure 5.14). This suggests that eddy diffusivity may be critical to the nature of density dependent fertilization effects.

5.4 DISCUSSION

These results have important implications for management measures to control COTS because they suggest that there may be a non-linear relationship between COTS density and zygote (larval) production, such that larval production increases faster than expected once density exceeds certain critical values. This means

that if COTS density can be maintained below certain critical levels , there is a substantially greater probability of recruitment failure because population-level reproductive output and the likelihood of further outbreaks declines more rapidly than indicated by density alone. The threshold level (level at which zygote production begins to rapidly increase) based on the simulations we have conducted here appears to be at spawning densities of around 13-18 adult (age 2+) COTS ha^{-1}, a threshold somewhat higher than those related to ecological thresholds for maintaining COTS populations or coral cover which are around 7-9 COTS ha^{-1} (sections 2, 3 above). COTS s populations were predicted on average to achieve 50% fertilization at densitie8-9 COTS ha^{-1}, more similar to our findings for other COTS outbreak thresholds as well as published values (Keesing and Lucas 1992).

The configuration of the model and its parameters has been well validated in terms of comparisons with experimental field trials (Babcock and Mundy 1993, Babcock et al. 1994). The pattern of increasing fertilisation success with increasing density is corroborated by observations of natural spawning (Babcock and Mundy 1993) during two separate natural spawnings of COTS at Davies Reef in 1990. In the first instance 88 starfish were observed spawning in a transect of approximately 200×10m, (440 ha^{-1}). Densities in surrounding areas were substantially lower than this (the transect was adjacent to a sandy lagoon area on one side), so the effective density was probably substantially lower than this. During this spawning eggs were sampled from several spawning females and an average fertilization rate of 83% was observed at the peak of the spawning. At the same site later in the month, eggs were sampled from a spawning female at the time three male starfish were observed spawning (spawning density of 20 ha^{-1}), and sampled eggs were observed to be fertilized at a rate of 23%.

Not all attempts to model population level effects of fertilization have revealed Allee effects in free spawning invertebrates. For example the studies of sea urchins (Lundquist and Botsford 2004) and scallops (Claerboudt 1999) found that the relationship between fertilization and population density was linear rather than exponential. While these models were similar to our simulation model, there were also some important differences: (1) they modelled other focal species; (2) their model areas were much smaller (5m x 5m, 10x10m) based on the fertilisation dynamics of their focal species, and they did not include boundary corrections; (3) they used a range of sperm dispersal distributions; and (4) in the case of Lundquist and Botsford (2004) the number of zygotes produced was calculated as the density of spawners multiplied by the mean percentage of eggs fertilised, whereas our model explicitly accounted for the total number of eggs produced as well as the resultant dispersion of the eggs and overlap with sperm concentrations. Neither of these studies were supported by parallel empirical validation. The study of Levitan and Young (1995) using the echinoid *Clypeaster rosaceus* was based on a series of laboratory and field experiments as well as population level simulation models that did predict Allee effects, and which were validated by the field experiments. These simulations were conducted across a very wide range of population sizes, spanning over 5 orders of magnitude, a factor which was instrumental in understanding the nature of density dependent effects in *Clypeaster*. Such factors may in part explain differences among the models above. For example, the lack of boundary corrections such as we have employed in the models (c.f. Lundquist and Botsford 2004, Claerboudt 1999) would effectively represent smaller populations and not include the effects of spawning taking place outside the box. Such effects are likely to be especially important when examining additive or multiplicative effects of multiple small increments in sperm concentration, as well as sperm-egg interactions over extended periods in the downstream.

Previous modelling studies have indicated that both the nature of density dependent effects (i.e. presence/absence of Allee effects), and the absolute values of fertilization or zygote production, can be critically influenced by a number of key parameters. In addition to spawner density, properties such as population size, level of aggregation, rate of sperm release have been highlighted as being particularly important (Levitan and Young 1995, Claerboudt 1999, Lundquist and Botsford 2004). In addition, sensitivity analyses conducted by us suggest that parameters such as eddy diffusivity (u*) may also critical to the nature of density dependent fertilization effects.

While the results of the current study are encouraging they are preliminary in that a number of these key parameters relating to the simulation of COTS fertilisation success could not be included in our models. Furthermore, while most of our parameters are based on direct measurement, a number have been obtained from the literature and are based on other species or other environments. These factors have the

potential to affect conclusions in relation to the overall nature of density dependent effects. Perhaps more importantly, they have the potential to affect the accuracy of quantitative predictions that are required in the case of practical application of any predicted reproductive density thresholds to the hands-on management of COTS (i.e. culling). The difference between 15, 10 or 5 COTS ha^{-1} will become increasingly critical as cost efficiency of manual injection declines at low densities, therefore further work to refine the model and obtain further measurements of a small set of key parameters is desirable.

It has not been possible to fully explore and simulate the sensitivity of COTS reproductive success to populations at a range of levels of aggregation. This is important because COTS are known to aggregate and this aggregation may increase during some spawning events (Babcock et al. 1994). Levels of aggregation may also affect the level of spawning synchrony (Okaji 1991). On reefs, spawning depth will also vary, and has the potential to affect fertilization rates as well but it has not been possible to include simulations of this variability. Also our simulations have been restricted to relatively low population sizes, large cell sizes, and small spatial extents due to time restrictions on this project. Sex ratios of COTS populations are also reported to vary (Pratchett et al 2014), but we have not been able to simulate variations in the relative numbers of male and female individuals. Some uncertainty also remains around the sperm release rate of COTS (c.f. Benzie and Dixon 1994) in relation to COTS fertilisation success suggesting further measurements may be required in order to reduce uncertainty in this area. Finally, some parameters we have used here (based on the work of Babcock et al. 1994) we have derived from literature values. Parameters such as u*, sperm density and sperm swimming speed could be measured directly in a relatively simple manner. Sperm swimming speeds can be used in alternative formulations of equations predicting sperm-egg interactions, allowing us to obtain more than one estimates of fertilization success based on predictions of gamete dispersion.

In summary, modelling of COTS population reproductive success suggests that there may be thresholds in reproductive success that could be used to achieve more effective management of COTS populations on the GBR. These applications could relate to both active management (culling) situations but also in the broader context of monitoring and awareness of incipient outbreak conditions. The quantitative accuracy of these thresholds is critical to their application within a comprehensive Integrated Management Framework and we suggest a discrete set of further modelling simulations and empirical measurements be completed to increase certainty around these thresholds.

Table 5.1 Summary of diffusion model parameters, values and sources.

Parameter	Value (units)	Source
x - distance parallel to current (i.e. downstream distance)	assigned (m)	Babcock et al. 1994
y - distance horizontal to current (i.e. cross-current direction)	assigned (m)	Babcock et al. 1994
z - distance vertical to current	assigned (m)	Babcock et al. 1994
S - sperm concentration	to be solved (m^{-3})	Babcock et al. 1994
E - egg concentration	to be solved (m^{-3})	Babcock et al. 1994
Q_s - sperm release rate	6.14×10^{8} ($sperm.sec^{-1}$)	Babcock et al. 1994
Q_e - egg release rate	10^{7} ($egg.sec^{-1}$)	Birkeland and Lucas 1990, Lucas 1986
$\bar{U}$ - mean current velocity	0.12 ($m.sec^{-1}$)	Babcock et al. 1994
δ_x, δ_y, δ_z - stc dev of diffusion in x,y,z axes	unitless	Babcock et al. 1994
h - height of sperm release	0.5 (m)	Babcock et al. 1994
d - total water depth	7 (m)	Babcock et al. 1994
B - rate parameter of plume spread	0.5 (unitless)	Babcock et al. 1994
u* - friction velocity	$\bar{U}$ × 0.05 - 0.1	Babcock et al. 1994, Babcock et al. 2000
αy - diffusion coefficient y axis	1.15 (unitless)	Babcock et al. 1994
αz - diffusion coefficient z axis	0.65 (unitless)	Babcock et al. 1994

Table 5.2 Fertilization Model parameters for an open system

Parameter	Value (unit)	Source
F- fertilization rate	To be solved	
θ - fertilization rate parameter	9.42×10^{10} (m^2; ≈3% x.s. egg area - 200 µm)	Babcock et al. 1994 - rate constant in closed vessel
t - time over which gametes interact	time step (sec)	Babcock et al. 1994
u_s* - sperm swimming speed	1.9×10^{-4} ($m.sec^{-1}$)	Levitan et al. 1991
ϕ_{cont} - egg target area	9.42×10^{-10} (m^2; 3% x.s. egg area - 200 µm)	Babcock et al. 1994, Denny and Shibata 1988

Table 5.3 Spawning Ecology parameters and sources

Parameter	Value	Source
$P_{♀}$ - spawning individuals	Max 0.68 (proportion)	Babcock et al. 1994
$N_{♀}$ - spawning events	2-4 (count)	Babcock et al. 1994
$S_{♀}$ - sex ratio	1:1	
T_v - duration of gamete viability	7200 (sec)	Benzie and Dixon 1994 (Fig 5e)
T_s - duration of spawning	1800 (sec)	Babcock et al. 1994

Table 5.4 Comparison of fits of linear, power and exponential functions for base-case fertilisation model (with u*=0.05) outputs of (A) fertilization success-COTS abundance and (B) zygote production-COTS abundance values, as well as Sensitivity scenario (with u*=0.10). The number of points n included = 58. The best fit model based on comparison of the sum of squares (SS) is shown in bold.

(A) Fertilisation success						
	Linear	**y=ax+b**	**Power**	**y=axb**	**Exponential**	**y=aebx**
	value	std	value	std	value	std
a	0.14	0.12	0.14	0.12	0.28	0.12
b	0.61	0.33	0.61	0.33	0.06	0.03
SS	0.171		**0.037**		0.460	
(B) Zygote production (base-case with u*=0.05)						
	Linear		**Power**		**Exponential**	
a	3419.4	0.0	608.6	0.0	5720.6	0.1
b	-6299.4	0.2	1.6	0.0	0.1	0.0
SS	2.37E+09		1.44E+09		**7.86E+08**	
(C) Zygote production sensitivity with u*=0.10						
	Linear		**Power**		**Exponential**	
a	1689.2	0.0	2263.2	0.1	6865.6	0.1
b	1459.8	0.2	0.9	0.0	0.1	0.0
SS	**3.92E+07**		4.84E+07		2.55E+08	

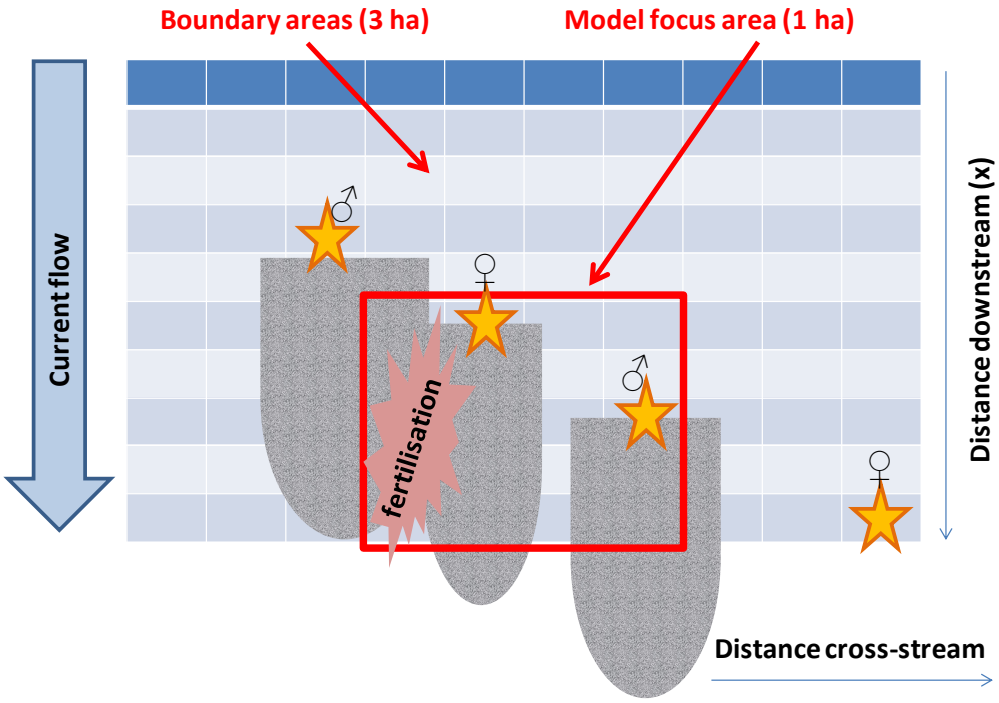

Figure 5.1 Schematic illustration of model structure (not to scale) showing male and female COTS spawners and sperm and egg downstream dispersion plumes.

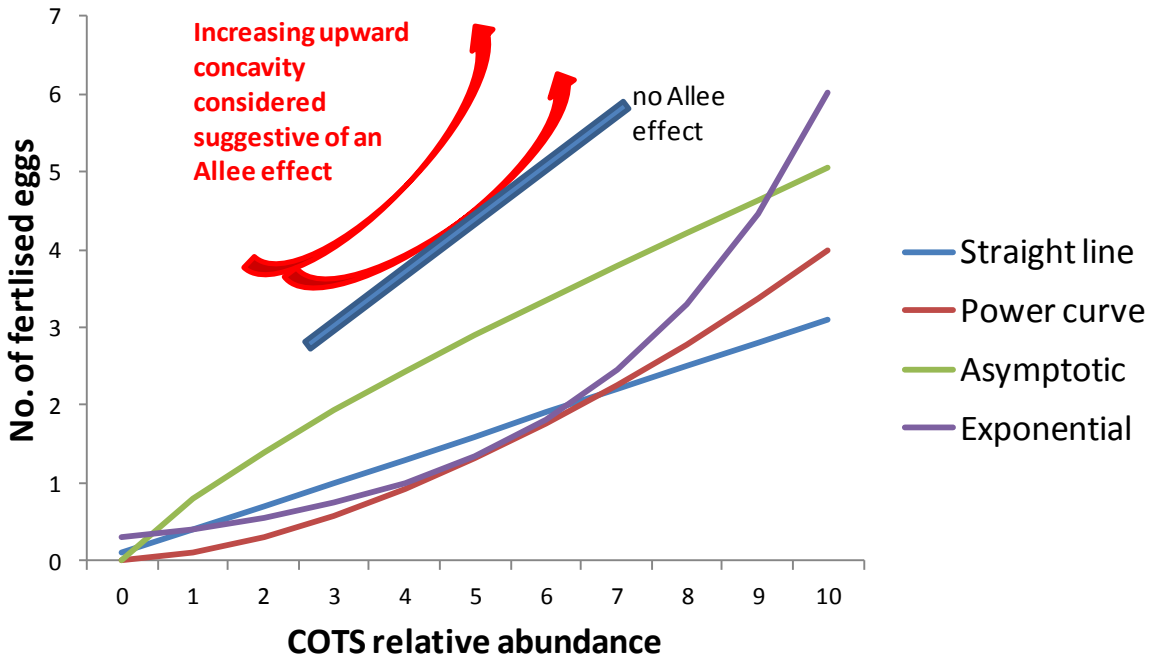

Figure 5.2 Schematic illustration of four different potential shapes of a recruitment curve for COTS at low stock abundance levels.

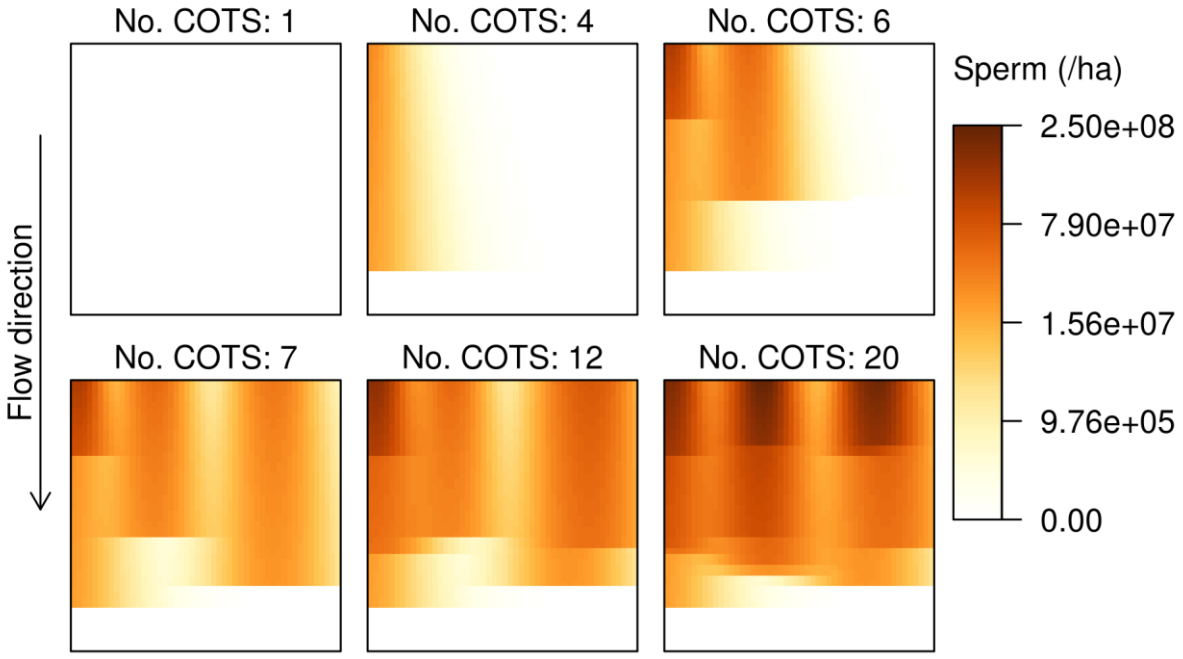

Figure 5.3 Sperm plumes over an area of one hectare with increasing numbers of initial COTS up to a total of 20.

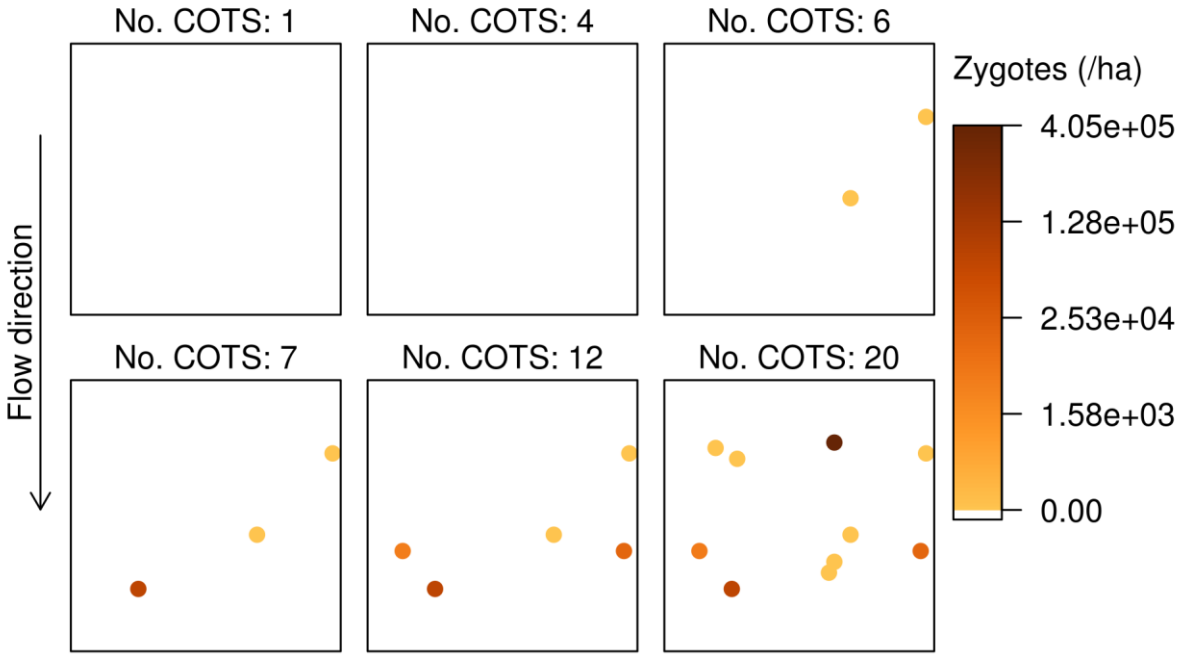

Figure 5.4 Zygote plumes over an area of one hectare with increasing numbers of initial COTS up to a total of 20.

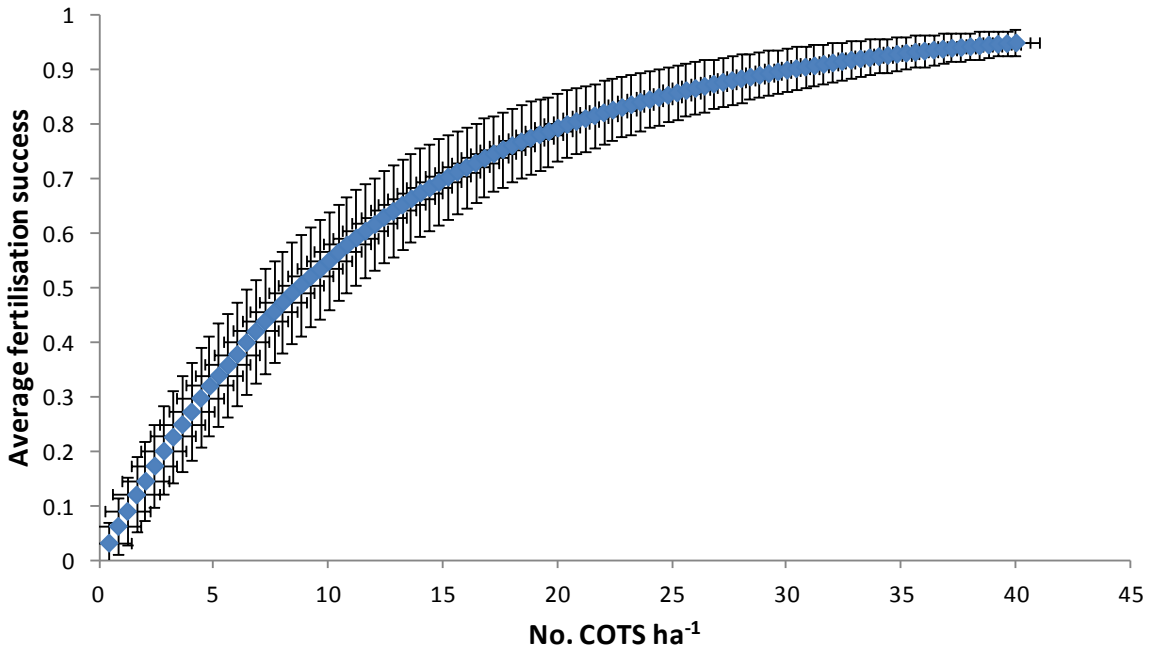

Figure 5.5 Model predicted average fertilization success (+1 std) from 2000 simulations of each of the COTS spawning densities as indicated, and when using the base-case model version.

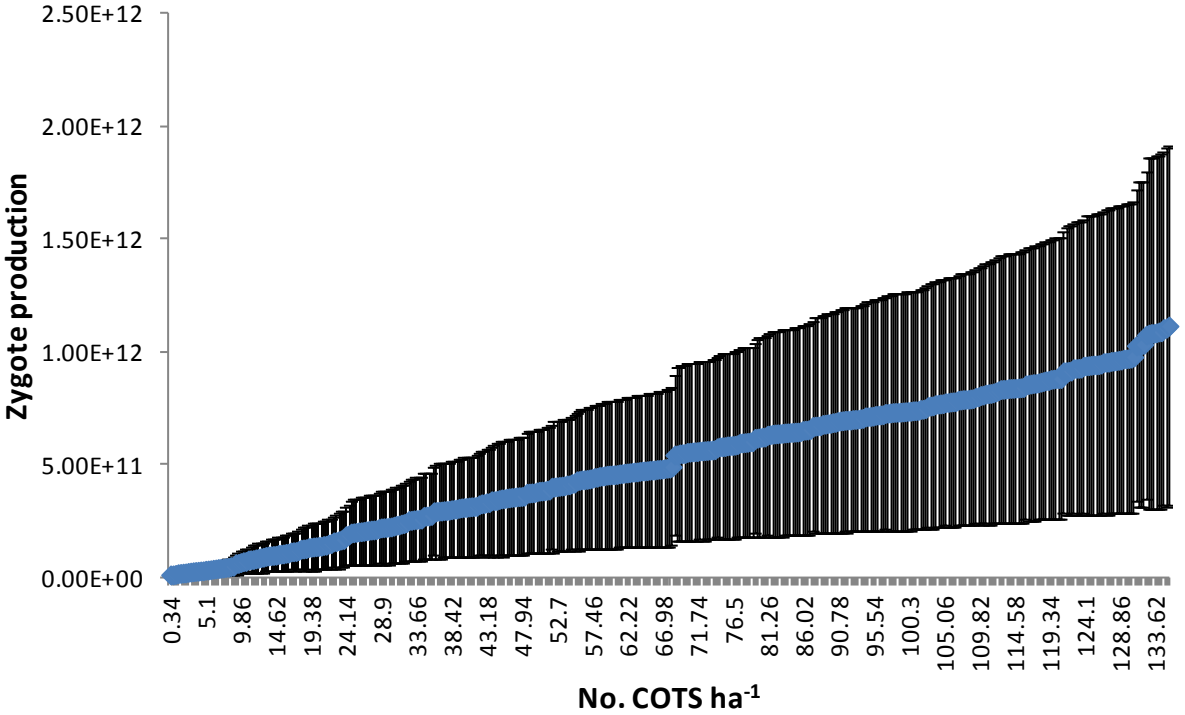

Figure 5.6 Model-predicted zygote production (+ std) from 2000 simulations as a function of COTS density shown from low densities up to high densities of 135 COTS ha^{-1}.

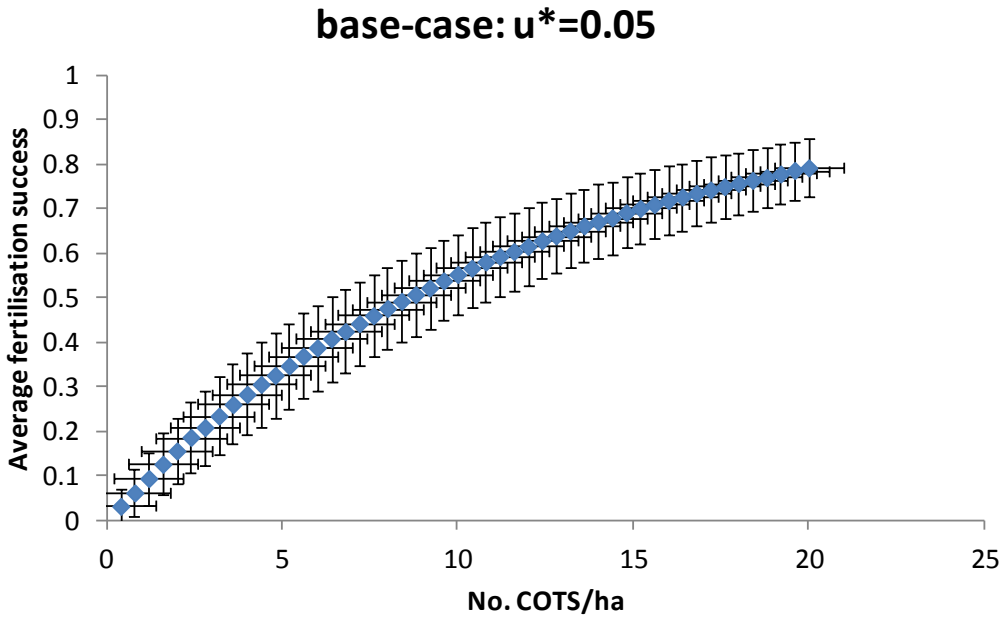

Figure 5.7 Higher resolution plot of fertilisation success rate as a function of COTS density, shown for lower values of COTS density up to 20 COTS ha^{-1}.

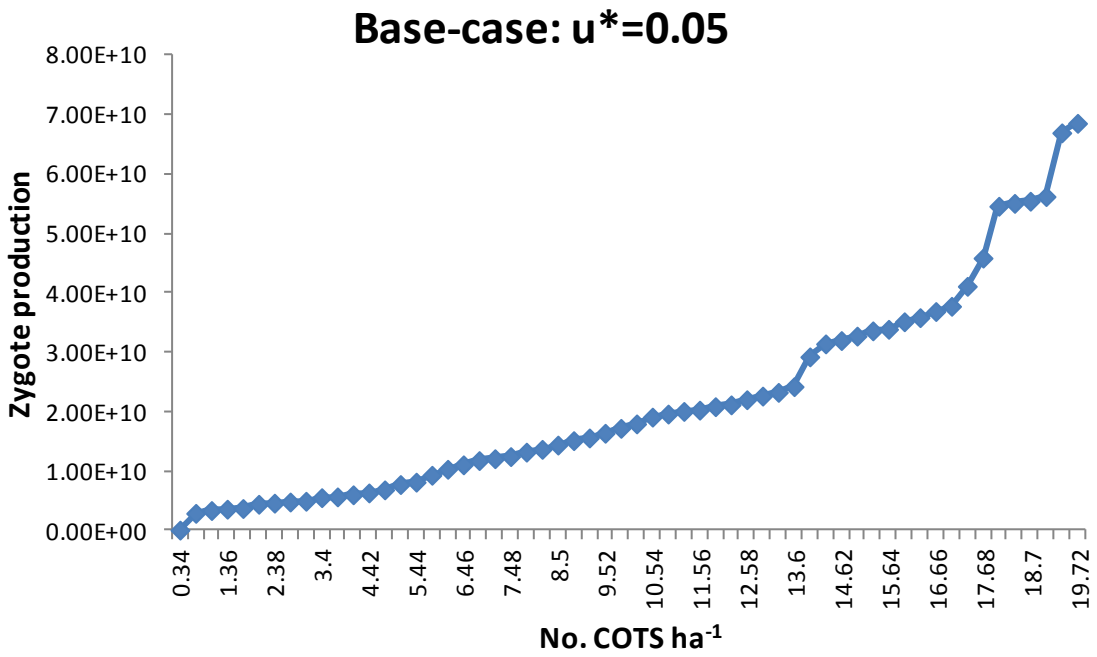

Figure 5.8 Higher resolution plot of zygote production as a function of COTS density, shown for lower values of COTS density up to 20 COTS ha^{-1}. The vertical arrows highlight threshold-type step changes in the relationship.

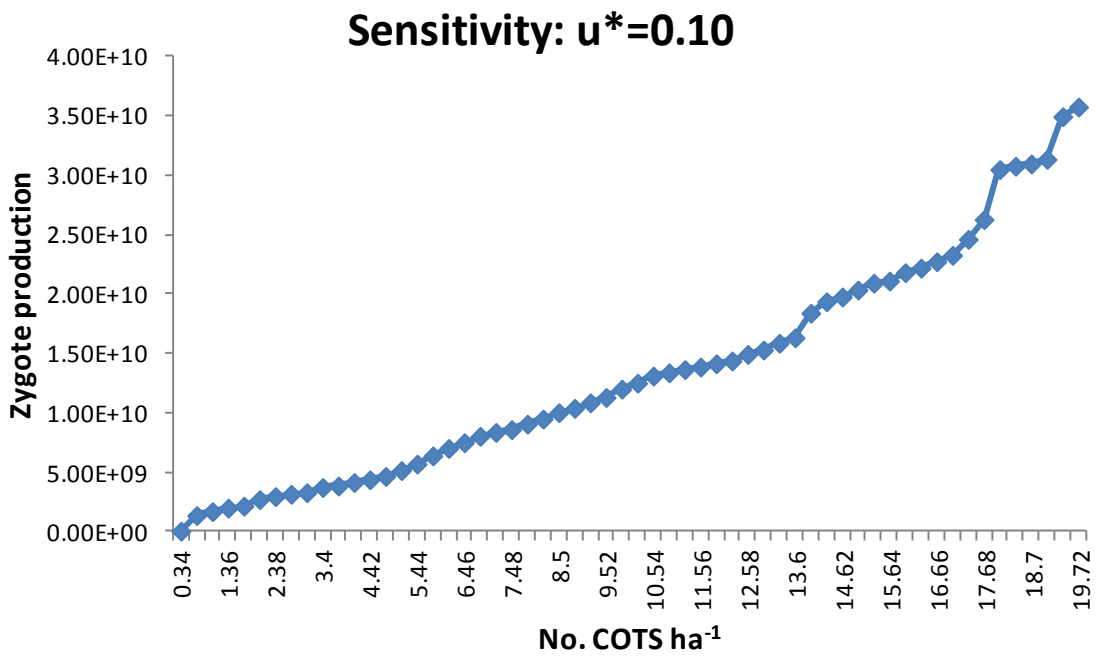

Figure 5.9 Zygote production as a function of COTS density when using a larger value for the parameter u*, shown for lower values of COTS density up to 20 COTS ha^{-1}.

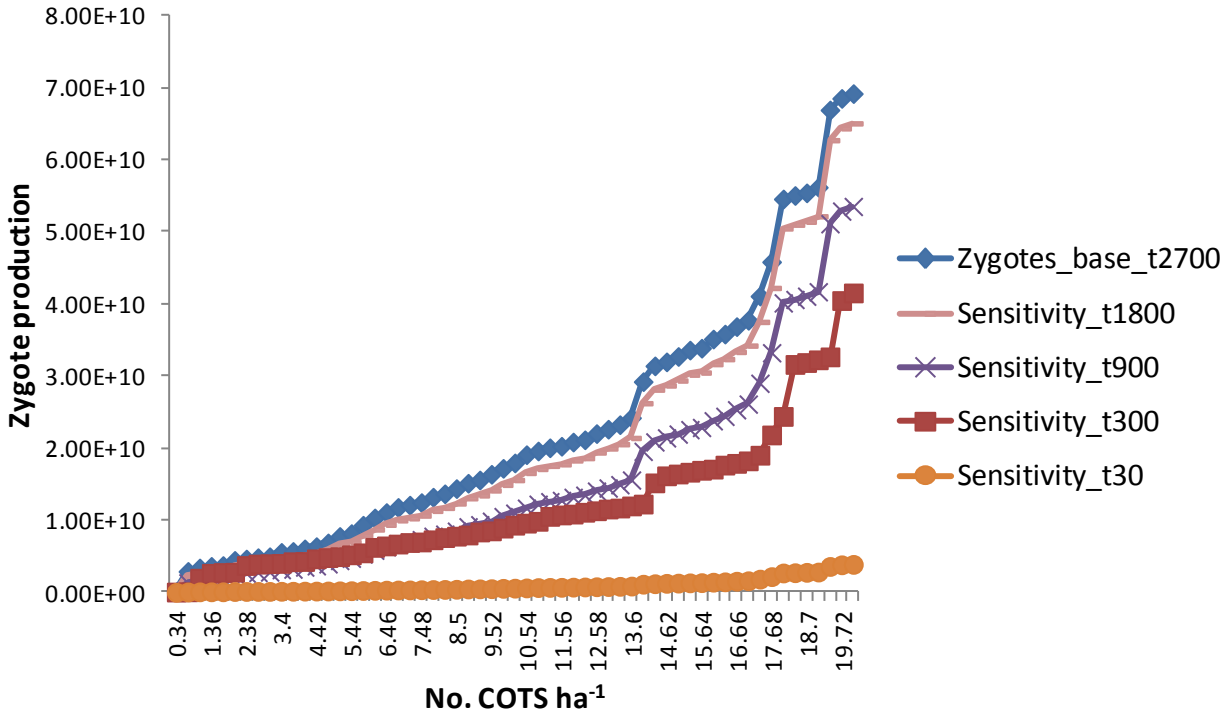

Figure 5.10 Sensitivity analysis showing zygote production as a function of COTS density for the base-case model with *t*=2700sec compared with lower settings of *t* as shown.

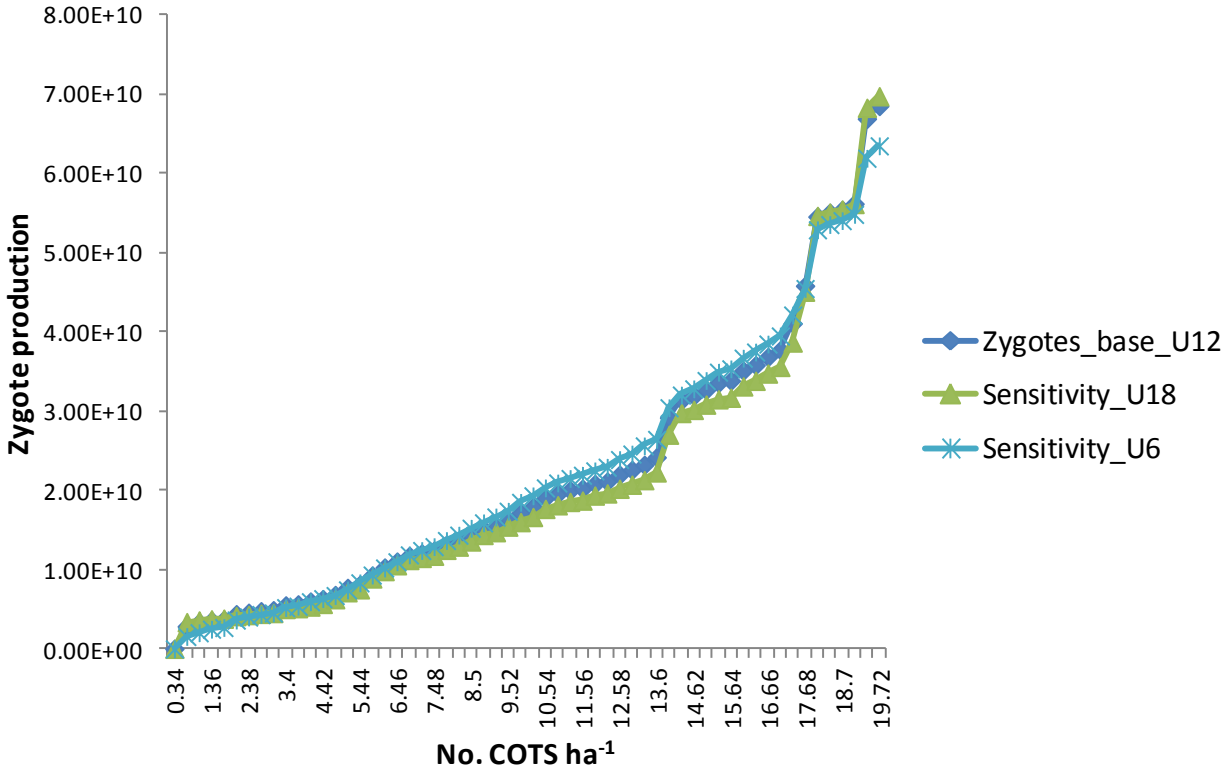

Figure 5.11 Sensitivity analysis showing zygote production as a function of COTS density for the base-case model with mean current velocity parameter *U*=0.12 m/s compared with a higher (0.18) and lower (0.06) value.

(A)

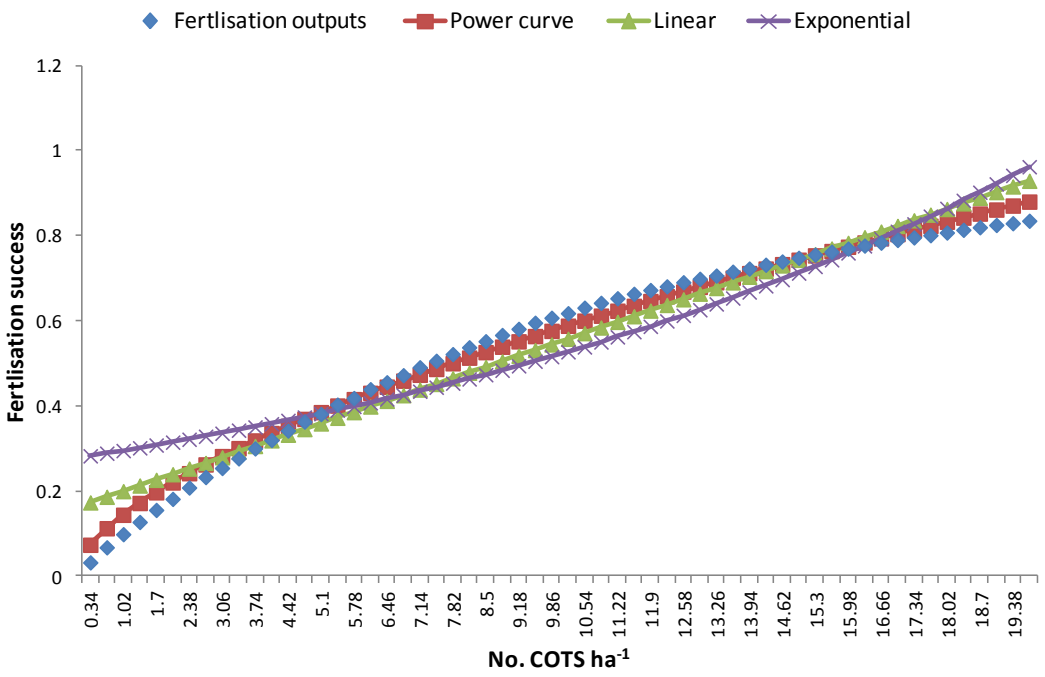

(B)

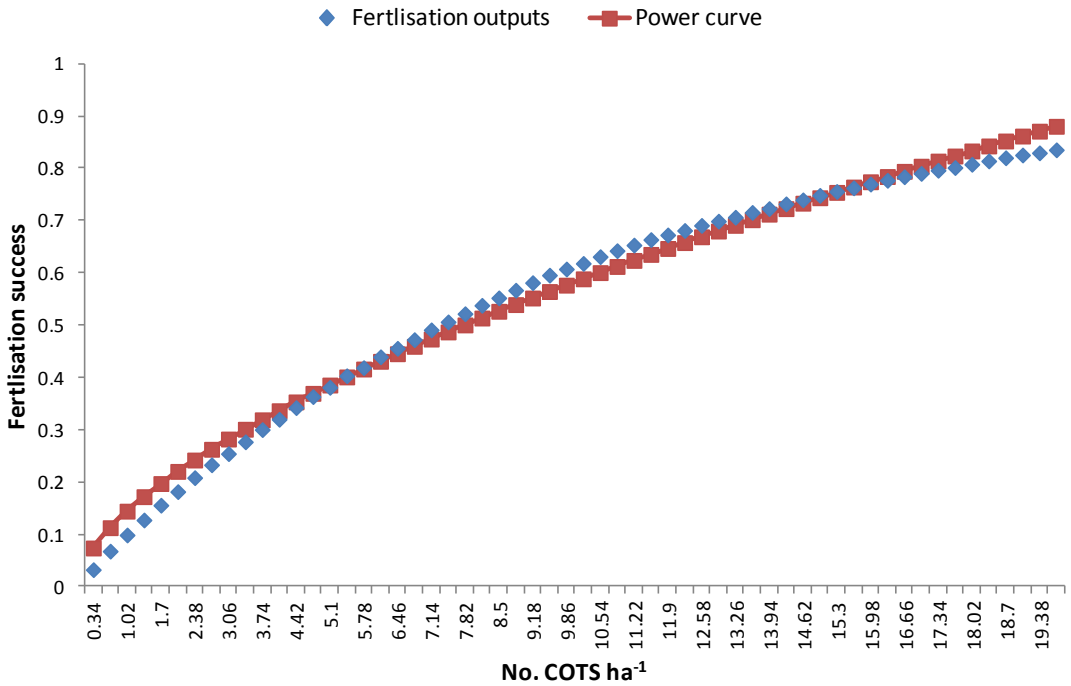

Figure 5.12 (A) Comparison of alternative fitted curves with fertilization success plotted as a function of COTS abundance. (B) Fertilisation model outputs shown plotted with best-fit power curve.

(A)

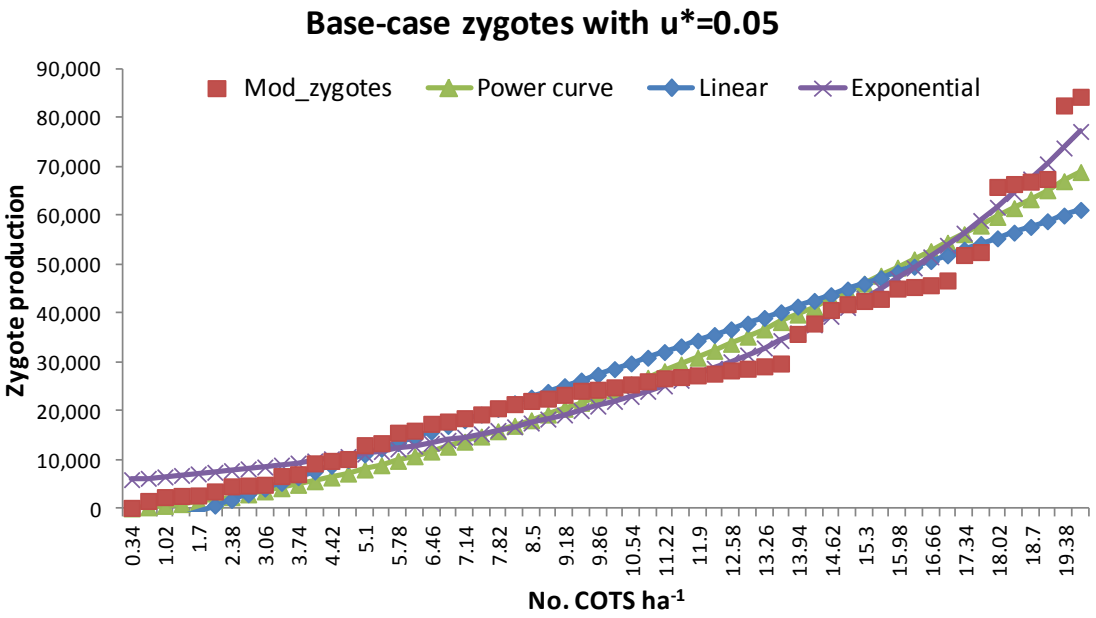

(B)

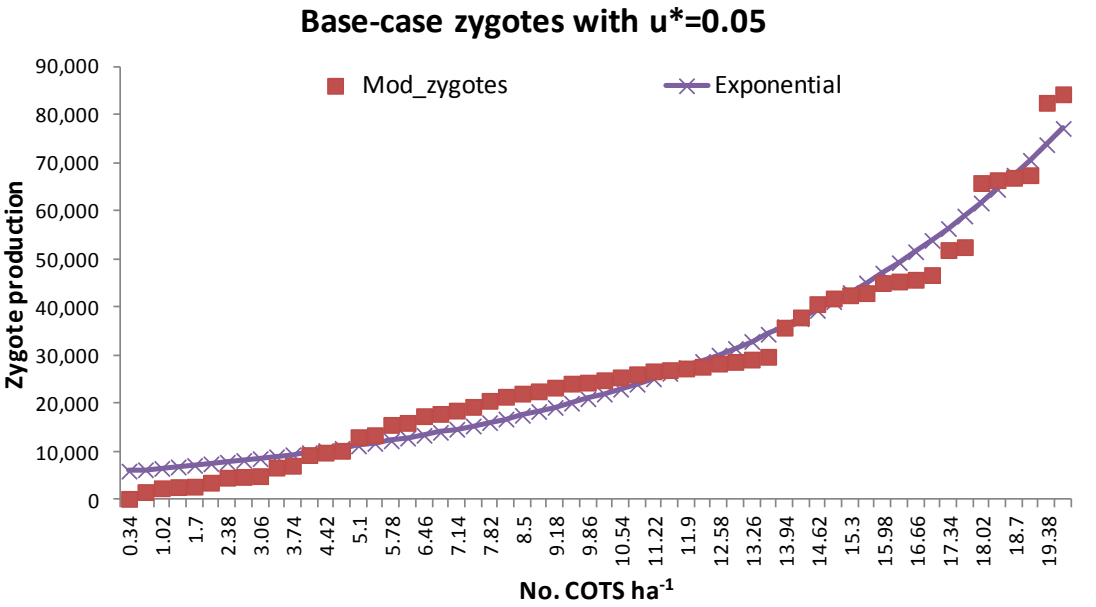

Figure 5.13 (A) Comparison of alternative fitted curves for base-case fertilisation model zygote production plotted as a function of COTS abundance. (B) Zygote production model outputs shown plotted with best-fit exponential curve

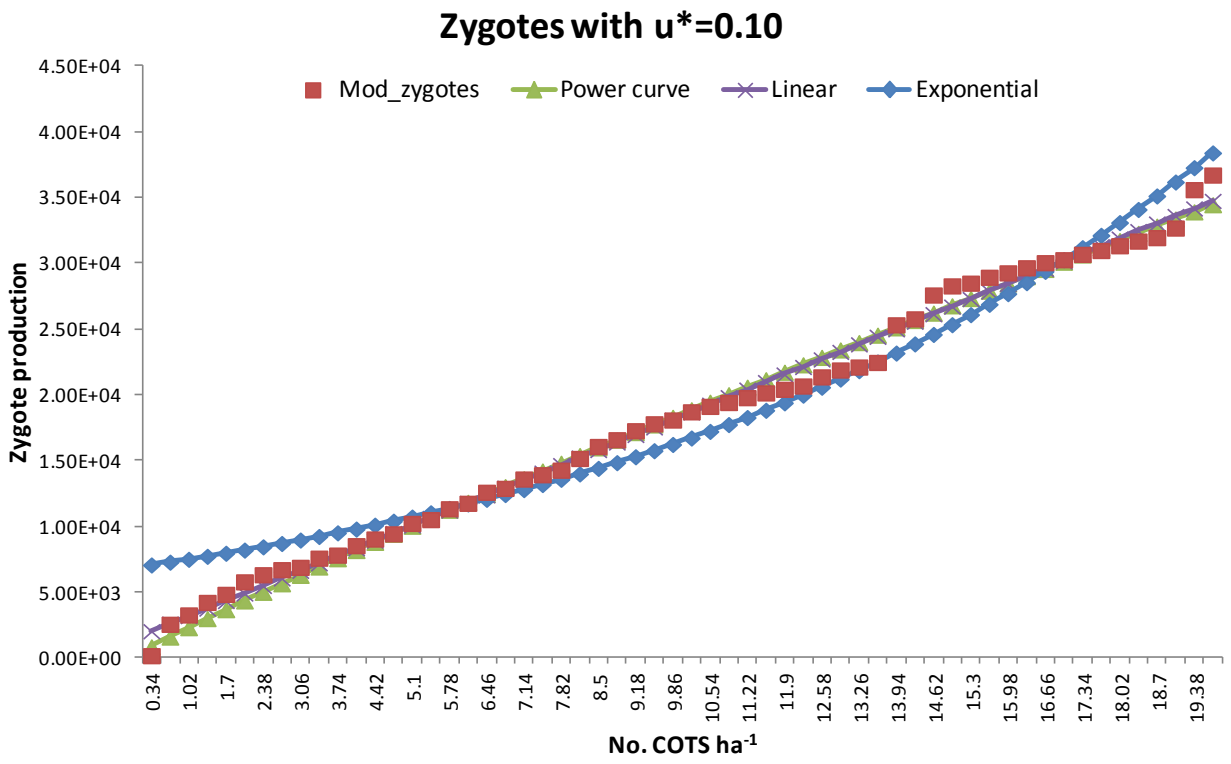

Figure 5.14 Comparison of alternative fitted curves for alternative fertilisation model (with u*=0.10) showing zygote production plotted as a function of COTS abundance.

6 Summary and future work

Using data collected at Lizard Island by Fisk and Power (1999) we developed a preliminary Catch-Per-Unit-Effort CPUE-COTS density equation that can be used to convert between estimates of COTS density and field observations of the numbers of COTS observed or culled per unit time. CPUE data can provide an index of the relative abundance of COTS in the field, but relating this directly to the underlying abundance or density of the population is confounded by the fact that this relationship is seldom linear, and factors such as handling time mean that a hyperstable relationship (i.e. the CPUE values start converging to some asymptotic value at high COTS densities) is more likely. Through statistically fitting to available data, we derived a preliminary relationship between COTS density and CPUE:

$$\mathrm{CPUE} = 0.669(N^{0.5})$$

Using the COTS management program cull data and our MICE model (Morello et al. in press), we estimated that the selectivity of the 1 year-old animals (those we classified as younger than 2 years) is 19%, i.e. on average, we estimate that divers find and remove 19% of these smaller/younger animals, and we use this to convert model CPUE estimates to equivalent field measurements.

The critical ecological threshold levels that are needed to completely collapse a COTS population were estimated as density of 7.1 (±2.3) 2+COTS ha^{-1} which equates to a COTS (removal) CPUE value of 0.028 (±0.01) 2+ COTS/min. This is the point at which there is an abrupt decline in COTS such that the population is unable to sustain itself, and occurs at a low coral cover of approximately 14%. In essence, if there is no control but COTS are at densities of 7.1/ha and there coral cover is below 14%, the COTS population will collapse because of starvation. This may relate to a range of factors such as that under these conditions there is little food for a growing population and low population densities may minimise the chance of successful reproduction.

The Morello et al. (in press) MICE model equations and best fit parameter estimates are used to solve for the number of COTS that keeps fast-growing coral in equilibrium at different coral cover levels showing that for fast-growing coral, there are trade-offs between the rate of growth of coral and the removal through grazing by COTS. The model steady state analysis suggests that if coral cover is high, then the same number of COTS will have less impact on the system than for lower levels of coral cover. These results are compared with the outbreak threshold (10 COTS Ha^{-1}) defined by Keesing and Lucas (1992) for cover of fast growing coral ('Coralf') in the range 20% to 50%, and there is excellent agreement between the results over this range of coral cover. For coral cover in the range 20-40%, our preliminary results suggest that the COTS CPUE should be maintained below approximately 0.08-0.10 COTS/min to keep the coral cover stable at its current level. The COTS management program average (+STD) coral cover is 35% (±17%) with range 3-88% suggesting that on average CPUE target rates should be less than 0.1 COTS/min (5.4 COTS ha^{-1}) of 2+ (> 15 cm) individuals and for low coral cover (<20%), CPUE target rates should be lower, down to around 0.06 COTS/min (9.4 COTS ha^{-1}) of 2+ (> 15 cm) individuals. This compares well with the current management rules being implemented as follows:

> Coral cover over 40% - keep CPUE <=0.1 COTS/min (this study suggests 0.07-0.09 COTS/min)
>
> Coral cover approaching 20%, keep CPUE <=0.05 COTS/min (this study suggests 0.04 COTS/min)

These results also provide scientific support for the current management program procedures which require a more stringent removal removed to (i.e. a lower CPUE rate) when coral cover is below rather than above 40%. Nevertheless at high levels of coral cover it may be desirable to reduce COTS densities well below the cover-specific definition of outbreak level, particularly where this may be at or above threshold levels of fertilization success or zygote production. This may have the benefit of inhibiting secondary outbreak and would need to be a factor in prioritization and triage around a regional COTS management program. Results are preliminary only at this stage and may be refined as further data and information become available.

A spatially expanded version of the Morello et al. (in press) COTS model was used to further explore these findings, showing that both the proportion of COTS removed and initial coral levels have a substantial effect on the average number of years taken for fast-growing coral to recover. Moreover, progressively increasing the proportion of COTS age 1 available for removal (i.e. the selectivity of age 1 COTS) and the proportion of total COTS removed (age 1 and age 2+ COTS), proportionally decreases the effects COTS have on coral. Future work should include an analysis of the total removals by size. This could be done by taking the Morello et al. (in press) model for Lizard Island, for example, including a six-monthly time step, reproducing the number of age classes represented and fitting the model to these age classes of the removals. In this way we would be able to use the model to simulate the removal of different age classes more reliably.

The work carried out in the first three sections of the report is based on data from many different sources. Some data, such as Fisk and Power (1999) are historical and not entirely applicable to the current situation for a number of reasons including the use of different, less efficient, removal methods compared to those used at present, as well as the limited spatial coverage of the removals. Owing to the fact that the data collected by Fisk and Power (1999) presented simultaneous quantification of both removals (CPUE) and density of COTS in the water (*N*), and were therefore more suited for the current analyses than the COTS management control data, i.e. to demonstrate the usefulness of field data towards calculating the CPUE-COTS relationship and applying it to translate model-based estimates of ecological thresholds to equivalent measures used by field practitioners. Similarly, some of the work is based on the data collected by the AIMS Long Term Monitoring Program (LTMP). Compared to the AIMS LTMP data, the GBRMPA Field Monitoring Program (FMP) data certainly appear to yield a more comprehensive estimate of COTS, but they do not cover the time series covered by the LTMP, especially in terms of capturing a complete COTS outbreak. For the purpose of fitting the MICE model to reproduce outbreak dynamics, therefore, the LTMP data were more relevant than the FMP data. In essence, the data available are plentiful and all of great value but, at the time of writing, comparability of datasets was not ideal and precluded the use of some datasets in certain analyses. This highlights that future efforts should be expended to accurately review all available COTS-related data towards informing and directing the collection of further data in the context of the form and extent of information already available as well as their possible use.

Results of models of reproductive success have important implications for management measures to control COTS because they suggest that there may be a non-linear relationship between COTS abundance and zygote (larval) production, such that larval production increases faster than expected once density exceeds certain critical values. This means that if COTS density can be reduced below certain critical levels, then there is a substantially greater probability of recruitment failure because of population level reproductive output, and the likelihood of further outbreaks, declines more rapidly than indicated by density alone. The threshold level for zygote production from the simulations we have conducted here appears to be at spawning densities of around 13-18 COTS ha^{-1}. This was slightly higher than threshold densities for maintenance of coral cover and for the ability of COTS populations to be sustained (sections 2 & 3 above, Keesing and Lucas 1992), however, 50% fertilization rates were predicted at densities of around 8-9 COTS ha^{-1}, a figure closer to thresholds from our work modelling critical ecological thresholds for controlling COTS.

While the results of the current study are encouraging they are preliminary in that a number of these key parameters relating to the simulation of COTS fertilization success could not be included in our models. Furthermore, while most of our parameters are based on direct measurement, a number have been obtained from the literature and are based on other species or other environments. These factors have the potential to affect conclusions in relation to the overall nature of density dependent effects. Perhaps more importantly, they have the potential to affect the accuracy of quantitative predictions that are required in the case of practical application of any predicted reproductive density thresholds to the hands-on management of COTS (i.e. culling). The difference between 15, 10 or 5 COTS ha^{-1} will become increasingly critical as cost efficiency of control declines at low densities, therefore further work to refine the model and obtain further measurements of a small set of key parameters is likely to be desirable.

In summary, modelling of COTS population reproductive success suggests that there may be thresholds in reproductive success that could be used to achieve more effective management of COTS populations on the GBR. These applications could relate to both active management (culling) situations but also in the

broader context of monitoring and awareness of incipient outbreak conditions. The quantitative accuracy of these thresholds is critical to their application and we suggest a discrete set of further modelling simulations and empirical measurements that would increase certainty around these thresholds.

Glossary

ADMB: Automatic Differentiation Model Builder, or AD Model Builder programming platform

AIMS: Australian Institute of Marine Science

AMPTO: Association of Marine Park Tourism Operators

Assessment: A mathematical population model coupled to a statistical estimation process that integrates data from a variety of sources to provide estimates of past and present abundance, fishing mortality and productivity of a resource

COTS: Crown of Thorns Starfish

CPUE: Catch Per Unit Effort

GBR: Great Barrier Reef, Australia

LTMP: Long Term Monitoring Program (AIMS)

MICE: Models of Intermediate Complexity for Ecosystem assessments

Model fitting: The process of statistically fitting (also called conditioning) a model to historical data

References

Ayling AM, Ayling AL. 1992. Discussion of the methodological problems associated with estimates of *Acanthaster planci* (Crown-of-thorns starfish) density on the GBR. http://www.searesearch.com.au/

Babcock RC, Mundy CN. 1992. Reproductive biology, spawning and field fertilization rates of *Acanthatser planci*. *Marine and Freshwater Research* 43:525-33

Babcock RC, Mundy CN. 1993. Seasonal changes in fertility and fecundity in *Acanthaster planci*. The possible causes and consequences of outbreaks of the crown-of-thorns starfish - Proceedings of a workshop. *7th International Coral Reef Symposium*, pp. 757-61. Guam, Micronesia

Babcock RC, Mundy CN, Whitehead D. 1994. Sperm Diffusion Models and In Situ Confirmation of Long-Distance Fertilization in the Free-Spawning Asteroid *Acanthaster planci*. *Biological Bulletin* 186:17-28

Benzie J, Black KP, Moran PJ, Dixon P. 1994. Small-Scale Dispersion of Eggs and Sperm of the Crown-of-Thorns Starfish (*Acanthaster planci*) in a Shallow Coral Reef Habitat. *The Biological Bulletin* 186:153-67

Benzie J, Dixon P. 1994. The Effects of Sperm Concentration, Sperm:Egg Ratio, and Gamete Age on Fertilization Success in Crown-of-Thorns Starfish (*Acanthaster planci*) in the Laboratory. *The Biological Bulletin* 186:139-52

Birkeland C. 1989. The Faustian traits of the crown-of-thorns starfish. *American scientist* 77:154-63

Birkeland C, Lucas JS. 1990. *Acanthaster planci: major management problem of coral reefs*. Boca Raton: CRC Press

Claereboudt M. 1999. Fertilization success in spatially distributed populations of benthic free-spawners: A simulation model. *Ecological Modelling* 121:221-33

Dana TF, Newman WA, Fager EW. 1972 Acanthaster aggregations: interpreted as primarily responses to natural phenomena. *Pacific Science* 26:355-72

Denny MW. 1988. *Biology and the Mechanics of the Wave-Swept Environment*. New Jersey: Princeton University Press

Fisk DA, Power MC. 1999. Development of cost-effective control strategies for Crown-of-Thorns Starfish, CRC Reef Research Centre, Townsville

Fournier DA, Skaug HJ, Ancheta J, Ianelli JN, Magnusson A, et al. 2012. AD Model Builder: using automatic differentiation for statistical inference of highly parameterized complex nonlinear models. *Optimization Methods and Software* 27:233-49

Keesing JK, Lucas JS. 1992. Field measurement of feeding and movement rates of the crown-of-thorns starfish *Acanthaster planci* (L.). *Journal of Experimental Marine Biology and Ecology* 156:89-104

Levitan DR. 1995. The ecology of fertilization in free-spawning invertebrates. In *Ecology of marine invertebrate larvae*, ed. L McEdward. Boca Raton: CRC Press

Levitan DR, Young CM. 1995. Reproductive success in large populations: empirical measures and theoretical predictions of fertilization in the sea biscuit *Clypeaster rosaceus*. *Journal of Experimental Marine Biology and Ecology* 190:221-41

Lucas J. 1986 The Crown of Thorns Starfish. *Oceanus* 29:55-64

Lundquist CJ, Botsford LW. 2004. Model projections of the fishery implications of the Allee effect in broadcast spawners. *Ecological Applications* 14:929-41

Moran P, De'ath G. 1992. Suitability of the manta tow technique for estimating relative and absolute abundances of crown-of-thorns starfish (*Acanthaster planci* L.) and corals. *Marine and Freshwater Research* 43:357-79

Moran PJ. 1986. The *Acanthaster* phenomenon. *Oceanography and Marine Biology: an Annual Review* 24:379-480

Morello EB, Plagányi ÉE, Babcock RC, Sweatman H, Hillary R, Punt A. In press. Modelling to manage and reduce Crown-of-Thorns Starfish outbreaks. *Marine Ecology Progress Series*

Mundy C, Babcock R, Ashworth I, Small J. 1994. A Portable, Discrete-Sampling Submersible Plankton Pump and Its Use in Sampling Starfish Eggs. *The Biological Bulletin* 186:168-71

Okaji K. 1991. Delayed spawning activity in individuals of *Acanthaster planci* in Okinawa. In *Biology of Echinodermata*, ed. Tea Yanagisawa, pp. 291–5. Rotterdam: Balkema

Pennington JT. 1985. The Ecology of Fertilisation of Echinoid Eggs: The Consequences of Sperm Dilution, Adult Aggregation, and Synchronous spawning. *The Biological Bulletin* 169:417-30

Plagányi, É., Punt, A., Hillary, R., Morello, E., Thebaud, O., Hutton, T., Pillans, R., Thorson, J., Fulton, E.A., Smith, A.D.T., Smith, F., Bayliss, P., Haywood, M., Lyne, V., Rothlisberg, P. 2014. Multi-species fisheries management and conservation: tactical applications using models of intermediate complexity. *Fish Fisherie*s 15:1-22

Plagányi ÉE, Ellis N, Blamey LK, Morello EB, Norman-Lopez A, et al. In press. Can models and observations help predict trophodynamically induced shifts in ecosystem state? *Marine Ecology Progress Series*

Pratchett M. 2005. Dynamics of an outbreak population of *Acanthaster planci* at Lizard Island, northern Great Barrier Reef (1995–1999). *Coral Reefs* 24:453-62

Pratchett M. 2010. Changes in coral assemblages during an outbreak of *Acanthaster planci* at Lizard Island, northern Great Barrier Reef (1995–1999). *Coral Reefs* 29:717-25

Pratchett, M.S., Caballes, C.F., Rivera-Posada, J.A., Sweatman, H.P.A. 2014. Limits to understanding and managing outbreaks of Crown-of-Thorns Starfish (*Acanthaster* spp). Oceanography and Marine Biology: An Annual Review, 52:133-200

Sweatman H, Cheal AJ, Coleman G, Emslie M, Johns K, et al. 2008. Long-term Monitoring of the Great Barrier Reef, Australian Institute of marine Sciences, Townsville

Vine PJ. 1973. Crown of thorns (*Acanthaster planci*) plagues: the natural causes theory. *Atoll Research Bulletin* 166:1-10

CONTACT US

t 1300 363 400
+61 3 9545 2176
e enquiries@csiro.au
w www.csiro.au

YOUR CSIRO

Australia is founding its future on science and innovation. Its national science agency, CSIRO, is a powerhouse of ideas, technologies and skills for building prosperity, growth, health and sustainability. It serves governments, industries, business and communities across the nation.

FOR FURTHER INFORMATION

CSIRO Marine and Atmospheric Research
Russ Babcock
t +61 7 3833 5904
e russ.babcock@csiro.au
w www.cmar.csiro.au

CSIRO Marine and Atmospheric Research
Eva Plaganyi
t +61 7 3833 5955
e eva.plaganyi-lloyd@csiro.au
w www.cmar.csiro.au